

# Renormalization approach to bound states

Steffen Sykora<sup>1\*</sup> and Tobias Meng<sup>1</sup>

<sup>1</sup> Institute for Theoretical Physics and Würzburg-Dresden Cluster of Excellence ct.qmat,  
Technische Universität Dresden, 01069 Dresden, Germany

\* steffen.sykora@tu-dresden.de

September 27, 2021

## Abstract

A new semi-analytical approach to bound states based on a unitary transformation of the Hamiltonian is presented. The method is applied to study the interaction between a superconductor and a quantum spin. Known results from the t-matrix method and numerical studies are reproduced. A uniform picture of the interplay between the Yu-Shiba-Rusinov (YSR) bound states and the Kondo singlet state is presented by revealing the structure of the quasiparticles in both phases. The method can straightforwardly be extended to study the topological properties of combined bound states in chains of magnetic impurities.

---

## Contents

<b>1</b>	<b>Introduction</b>	<b>2</b>
<b>2</b>	<b>Non-magnetic impurity</b>	<b>3</b>
2.1	Theoretical approach to bound states	3
2.2	Spectral function	7
<b>3</b>	<b>Magnetic impurity in a superconductor</b>	<b>9</b>
3.1	Classical spin	9
3.1.1	Exact solution of the scattering problem	10
3.1.2	Spectral function	13
3.2	Quantum spin	14
3.2.1	Approximate solution of the scattering problem	15
3.2.2	Transformation of operators	20
3.2.3	Discussion of the quasiparticle nature	21
3.2.4	Spectral function	22
<b>4</b>	<b>Conclusion</b>	<b>23</b>
<b>A</b>	<b>Effect of spin and temperature</b>	<b>24</b>
	<b>References</b>	<b>25</b>

---

# 1 Introduction

The study of bound states at low temperature has become important for the understanding of the interaction between impurities and electronic properties of the underlying correlated material. An important example in this context is a magnetic impurity which interacts with a superconducting condensate leading to competition between the Yu-Shiba-Rusinov (YSR) bound states [1–3] and the Kondo physics [4–6]. Depending on the strength of the exchange coupling a transition from a regime with weakly coupled YSR states to a Kondo singlet state is found [7–9]. The formation of these bound states has been visualized by measurements of the spectral function using scanning tunneling spectroscopy [10–12].

The extension of these systems to more than one local moment gives rise to models of molecules [13–16] and spin chains [17, 18]. These systems have become particularly interesting both from the experimental and the theoretical side as they show properties of topological superconductivity and Majorana zero modes [19, 20]. Here the influence of the quantum nature of the impurity spin is expected to be of particular importance. The theoretical treatment of such systems therefore requires true many-body approaches that properly take into account the quantum nature of the local spin.

In recent years, some powerful theoretical methods like mean field calculations [7, 21], perturbation theory [22, 23], self-consistent approaches [24, 25] and the numerical renormalization group (NRG) approach [26–28] have been applied to study the formation of bound states in correlated systems. Usually the applicability of such methods is restricted to only one single impurity or to very small system sizes. In contrast, powerful analytical approaches which are able to tackle more than one impurity in an environment of a condensate in the thermodynamic limit are not available so far. Such an approach would allow for a deeper understanding of the underlying physical processes and the structure of the quasiparticle which is responsible for the bound state. In addition, the quantum nature of the local impurity is often important for the properties of the spectral function.

Motivated by these aims we have developed a new renormalization scheme for Hamiltonians with an interaction between a local moment and a superconducting condensate. Our diagonalization method shares some basic concepts with the known renormalization schemes for Hamiltonians [29–31]. Instead of eliminating the interaction part in a sequence of small steps, however, we propose a method that merely applies a single unitary transformation. A schematic picture of the method is shown in Fig. 1. The bound state appears as a singularity in the unitary transformation and an additional local contribution to the quasiparticle. Its energy is obtained from a renormalization of one single state of the conduction electron band. Due to the semi-analytical nature of our method and the readily generalizable unitary transformations used to diagonalize the Hamiltonian, also more than one impurity can in principle be implemented, and the quantum nature of the impurity is properly taken into account.

The rest of the paper is organized as follows. In Sec. 2 we introduce our method for the case of a non-magnetic impurity. We derive self-consistent equations for solving the scattering problem and show numerical results of the one-particle spectral function. Next, in Sec. 3 we apply the developed concepts to the problem of a magnetic impurity in a superconductor where we at first consider in Sec. 3.1 the exactly solvable problem of a classical spin. Known results of the YSR bound state are reproduced. Then, in Sec. 3.2 we generalize our method to a quantum spin and show numerical results for the one-particle spectral function in the weak and strong coupling regimes where we also discuss the nature of the bound state quasiparticle. Finally, a conclusion is

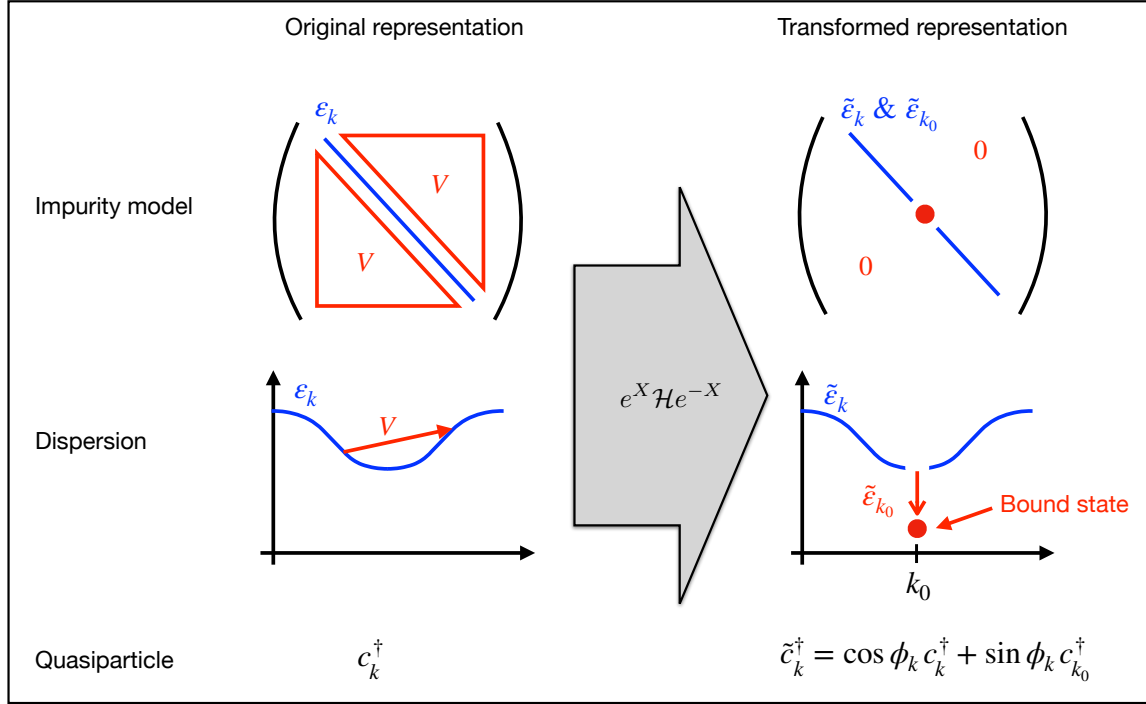


Figure 1: Schematic picture of our theoretical approach to bound states. The scattering term of the original Hamiltonian is eliminated by a unitary transformation  $e^X$ . This technique diagonalizes the Hamiltonian and generates a bound state at a momentum  $k_0$  (red dot) which is renormalized in energy. Excitations split into a coherent part and a local excitation.

given in Sec. 4.

## 2 Non-magnetic impurity

Before analyzing spinful impurities in  $s$ -wave superconductors, we explain our approach to bound states by applying it to the perhaps most simple case of a local potential impurity embedded into a spinless, normal-state electron system. Concretely, we consider a toy-model Hamiltonian  $\mathcal{H}_V$  composed of an electron-part  $\mathcal{H}_0$  and the electron-impurity-part  $\mathcal{H}_{1,V}$  proportional to the coupling strength  $V$ ,

$$\mathcal{H}_V = \mathcal{H}_0 + \mathcal{H}_{1,V} \quad \text{with} \quad \mathcal{H}_0 = \sum_k \epsilon_k c_k^\dagger c_k \quad \text{and} \quad \mathcal{H}_{1,V} = \frac{V}{2N} \sum_{k \neq k'} (c_k^\dagger c_{k'} + c_{k'}^\dagger c_k). \quad (1)$$

Here,  $\epsilon_k$  is the bare electronic dispersion, which is a function of the one-dimensional momentum  $k$ , and the lattice consists of  $N$  sites.

### 2.1 Theoretical approach to bound states

Following the idea of Ref. [31], we subject the Hamiltonian (1) to an exact mapping that brings the Hamiltonian to a new form  $\tilde{\mathcal{H}}_V$ . The mapping between the original Hamiltonian  $\mathcal{H}_V$  and  $\tilde{\mathcal{H}}_V$

is implemented by a unitary transformation,

$$\tilde{\mathcal{H}}_V = e^{X_V} \mathcal{H}_V e^{-X_V}, \quad (2)$$

where the hermiticity of  $\tilde{\mathcal{H}}_V$  requires  $X_V^\dagger = -X_V$ . For the operators, this implies

$$\tilde{c}_{k,V}^\dagger = e^{X_V} c_k^\dagger e^{-X_V}. \quad (3)$$

The transformed Hamiltonian should not only be quadratic in the original fermionic operators  $c_k^\dagger$ , but also have the diagonal form  $\tilde{\mathcal{H}}_V = \sum_k \tilde{\varepsilon}_k c_k^\dagger c_k$  with a renormalized dispersion  $\tilde{\varepsilon}_k$ . Note that such a treatment is not a usual diagonalization where the fermion operators in the Hamiltonian are rotated in the operator subspace. In our approach, the one-particle operators are kept in their original basis while the Hamiltonian is renormalized. Therefore,  $\tilde{\mathcal{H}}_V$  differs from  $\mathcal{H}_V$  (but it has the same eigenvalue spectrum as the original model).

As we explain below, a convenient ansatz for  $X_V$  is

$$X_V = \frac{1}{N} \sum_{k \neq k'} \frac{A_{k,V}}{\tilde{\varepsilon}_k - \tilde{\varepsilon}_{k'}} (c_k^\dagger c_{k'} - c_{k'}^\dagger c_k). \quad (4)$$

The real coefficients  $A_{k,V}$  will turn out to be key in the description of bound states. To determine their values, we plug the ansatz (4) into Eq. (2), which allows to determine  $A_{k,V}$  from the expansion of Eq. (2) in terms of commutators,

$$\tilde{\mathcal{H}}_V = \mathcal{H}_V + \frac{1}{1!} [X_V, \mathcal{H}_V] + \frac{1}{2!} [X_V, [X_V, \mathcal{H}_V]] + \dots \quad (5)$$

Up to first order in the generator  $X_V$ , the commutators of  $X_V$  with  $\mathcal{H}_0$  and  $\mathcal{H}_{1,V}$  as defined in Eq. (1) read,

$$\begin{aligned} [X_V, \mathcal{H}_0] &= -\frac{1}{N} \sum_{k \neq k'} A_{k,V} \frac{\varepsilon_k - \varepsilon_{k'}}{\tilde{\varepsilon}_k - \tilde{\varepsilon}_{k'}} (c_k^\dagger c_{k'} + c_{k'}^\dagger c_k), \\ [X_V, \mathcal{H}_{1,V}] &= \frac{V}{N^2} \sum_{kk'} \sum_{q(\neq k)} \frac{A_{k,V} + A_{q,V}}{\tilde{\varepsilon}_k - \tilde{\varepsilon}_q} (c_k^\dagger c_{k'} + c_{k'}^\dagger c_k). \end{aligned} \quad (6)$$

Since the scattering potential  $V$  is momentum-independent, one might also expect the coefficients  $A_{k,V}$  to be momentum-independent. As we will show below, however, that is not the full story. Instead,  $A_{k,V}$  can become singular at specific values of  $k$ , which indicates the formation of a bound state as we will show below. Furthermore, we will show that a singularity of  $A_{k,V}$  entails a renormalization of the one-particle energy from the bare value  $\varepsilon_k$  to a new value  $\tilde{\varepsilon}_k$  – but *only* at the  $k$  for which  $A_{k,V}$  is singular. This renormalization will be related to the binding energy of the bound state.

Using Eq. (6), we now evaluate all further higher order commutators and sum these terms up to infinite order using Eq. (5). We obtain the following expression for the renormalized Hamiltonian,

$$\begin{aligned} \tilde{\mathcal{H}}_V &= \sum_k \varepsilon_k c_k^\dagger c_k + \frac{V}{2N^2} \sum_k \left( \sum_{q(\neq k)} \frac{A_{k,V} + A_{q,V}}{\tilde{\varepsilon}_k - \tilde{\varepsilon}_q} \right) c_k^\dagger c_k \\ &+ \frac{1}{N} \sum_{k' \neq k} \left( \frac{V}{2} \cos \phi_{k,V} - A_{k,V} \frac{\sin \phi_{k,V}}{\phi_{k,V}} \right) (c_k^\dagger c_{k'} + c_{k'}^\dagger c_k) \\ &+ \frac{1}{N^2} \sum_{k' \neq k} \sum_{q(\neq k)} \frac{A_{k,V} + A_{q,V}}{\tilde{\varepsilon}_k - \tilde{\varepsilon}_q} \left( V \frac{\sin \phi_{k,V}}{\phi_{k,V}} + 2A_{q,V} \frac{\cos \phi_{k,V} - 1}{\phi_{k,V}^2} \right) (c_k^\dagger c_{k'} + c_{k'}^\dagger c_k), \end{aligned} \quad (7)$$

where we have introduced the dimensionless coefficient

$$\phi_{k,V} = \frac{1}{N} \sqrt{\sum_{q(\neq k)} \left( \frac{V/2 + A_{q,V}}{\tilde{\varepsilon}_k - \tilde{\varepsilon}_q} \right)^2}, \quad (8)$$

which plays the role of a  $k$ -dependent phase. The coefficients  $A_{k,V}$  are then determined by the condition that all non-diagonal scattering terms in Eq. (7) must vanish (i.e. terms combining *different* momenta  $k \neq k'$ ). This is done by an iterative numerical procedure that stops once all  $A_{k,V}$  are converged.

Consider the system for concreteness to contain only one impurity, in which case we expect (at most) a single bound state. Numerically, we then find that there is indeed a single momentum  $k_0$  at which  $A_{k_0,V}$  is singular (diverges as  $\sim N$ ). For all other momenta  $q \neq k_0$ , the coefficients are found to take the non-singular value  $A_{q,V} = V/2$ . In addition, the energies  $\tilde{\varepsilon}_q$  remain at their bare values,  $\tilde{\varepsilon}_q = \varepsilon_q$  for  $q \neq k_0$ .

To motivate the above numerical solution, we now show that it is self-consistent. We start with the ‘‘momentum’’  $k_0$  (to be determined) at which the bound state forms. Note that after the transformation, the quantum number  $k$  does not necessarily correspond to a physical momentum anymore – although we will see that this is essentially the correct interpretation for all values of  $k$  except  $k_0$ . Quite generally, the value of  $A_{k,V}$  is determined by the second and third line of Eq. (7). For the yet unknown momentum  $k_0$  at which  $A_{k_0,V}$  diverges, the phase

$$\phi_{k_0,V} = \frac{1}{N} \sqrt{\sum_{q(\neq k_0)} \left( \frac{V/2 + A_{q,V}}{\tilde{\varepsilon}_{k_0} - \tilde{\varepsilon}_q} \right)^2}, \quad (9)$$

remains very small ( $\propto 1/\sqrt{N}$ ) since the singular  $A_{k_0,V}$  is excluded from the summation over  $q$  (we recall our numerical results  $A_{q,V} = V/2$  and  $\tilde{\varepsilon}_q = \varepsilon_q$  for  $q \neq k_0$ ). Thus, we are allowed to expand the sin- and cos-functions in Eq. (7) up to lowest order. Given the singularity of  $A_{k_0,V}$ , and taking the limit of large  $N$ , this leads to

$$\frac{V}{2} - A_{k_0,V} + \frac{V}{2N} \sum_{q(\neq k_0)} \frac{A_{k_0,V}}{\tilde{\varepsilon}_{k_0} - \varepsilon_q} = 0. \quad (10)$$

Solving this equation for  $A_{k_0,V}$ , we obtain

$$A_{k_0,V} = \frac{V/2}{1 - \frac{1}{N} \sum_{q(\neq k_0)} \frac{V/2}{\tilde{\varepsilon}_{k_0} - \varepsilon_q}}. \quad (11)$$

For our solution to be self-consistent, we next need to show that the denominator may indeed become very small for particular values of the energy  $\tilde{\varepsilon}_{k_0}$ . The energy  $\tilde{\varepsilon}_{k_0}$  of the state  $k_0$  is in turn determined by evaluation of the corresponding renormalization equation. For a general  $\tilde{\varepsilon}_k$ , this renormalization equation is found from the contributions in the first line of Eq. (7). Comparing these contributions with the desired form  $\tilde{\mathcal{H}}_V = \sum_k \tilde{\varepsilon}_k c_k^\dagger c_k$ , we find

$$\tilde{\varepsilon}_k = \varepsilon_k + \frac{V}{2N^2} \sum_{q(\neq k)} \frac{A_{k,V} + A_{q,V}}{\tilde{\varepsilon}_k - \tilde{\varepsilon}_q}. \quad (12)$$

Except for the particular  $k = k_0$  where  $A_k$  becomes singular, the energy renormalization is  $\propto 1/N$  and thus negligible in the thermodynamic limit, i.e.  $\tilde{\varepsilon}_k = \varepsilon_k$  for  $k \neq k_0$ . The fact that states with  $k \neq k_0$  keep their energy means that those states may still be interpreted as states in the conduction band, with  $k$  playing the role of a physical momentum. For  $k = k_0$ , on the contrary, we find the renormalized energy  $\tilde{\varepsilon}_{k_0}$  to read

$$\tilde{\varepsilon}_{k_0} = \varepsilon_{k_0} + \frac{V}{2N^2} \sum_{q(\neq k_0)} \frac{A_{k_0,V}}{\tilde{\varepsilon}_{k_0} - \varepsilon_q}. \quad (13)$$

The renormalization is now finite because both the sum over states  $q$  and  $A_{k_0,V}$  yield a factor of  $N$ . Numerically, we find that  $k_0$  is located either at the bottom or top of the bare electronic band structure. This makes sense since the denominator in Eq. (13) then has a uniform sign, while divergent contributions of positive and negative signs cancel otherwise.

To find a solution of Eq. (13), we propose that  $\frac{1}{2N} \sum_q V/(\tilde{\varepsilon}_{k_0} - \varepsilon_q) \rightarrow 1$ , which is the condition for  $A_{k_0,V}$  to become singular according to Eq. (11). Using this claim and the explicit expression (11) in Eq. (13), we find

$$\tilde{\varepsilon}_{k_0} = \varepsilon_{k_0} + \frac{A_{k_0,V}}{N} = \varepsilon_{k_0} + \frac{1}{N} \frac{V/2}{1 - \frac{1}{N} \sum_{q(\neq k_0)} \frac{V/2}{\tilde{\varepsilon}_{k_0} - \varepsilon_q}}. \quad (14)$$

Solving this equation for the expression  $\frac{1}{2N} \sum_q V/(\tilde{\varepsilon}_{k_0} - \varepsilon_q)$  we obtain

$$\frac{1}{2N} \sum_{q(\neq k_0)} \frac{V}{\tilde{\varepsilon}_{k_0} - \varepsilon_q} = 1 - \frac{1}{2N} \frac{V}{\tilde{\varepsilon}_{k_0} - \varepsilon_{k_0}}. \quad (15)$$

Thus, in the thermodynamic limit the right hand side approaches '1' which is consistent with the above claim. Consequently, the solution of the renormalization equation (13) leading to the energy  $\tilde{\varepsilon}_{k_0}$  of the bound state is given by the equation,

$$\frac{V}{2N} \sum_{q(\neq k_0)} \frac{1}{\tilde{\varepsilon}_{k_0} - \varepsilon_q} = 1, \quad (16)$$

which exactly agrees with the result of the well known t-matrix approach to bound states [32]. The bound state energy is calculated by evaluating the momentum sum using the density of states of the free system and solving the resulting equation for  $\tilde{\varepsilon}_{k_0}$ . Usually the energy value  $\tilde{\varepsilon}_{k_0}$  lies below the bottom of the conduction electron band and it only exists if  $V < 0$ , i.e. in the case of an attractive scattering potential.

Finally, using Eq. (16) and solving Eq. (13) for  $A_{k_0,V}$  we obtain an explicit expression for the coefficient  $A_{k_0,V}$ ,

$$A_{k_0,V} = N(\tilde{\varepsilon}_{k_0} - \varepsilon_{k_0}), \quad (17)$$

which – as we found numerically – is proportional to  $N$  and thus becomes singular in the thermodynamic limit.

Next, we study the coefficients  $A_{k,V}$  and  $\phi_{k,V}$  for the fermionic states away from the singularity, i.e. with  $k \neq k_0$ . We again use the condition that all Hamiltonian matrix elements with  $k \neq k'$  in Eq. (7) must vanish. Now, the states with  $k \neq k_0$  are somewhere within the conduction band (not at its top or bottom), and we numerically find that the third line of Eq. (7) is negligibly small due

to the cancellation of contributions with different signs in the summation. Using Eq. (8) and the numerical result  $A_{k,V} = V/2$ , the second line of Eq. (7) yields

$$\tan \phi_{k,V} = \frac{1}{N} \sqrt{\sum_{q(\neq k)} \left( \frac{V/2 + A_{q,V}}{\varepsilon_k - \varepsilon_q} \right)^2}. \quad (18)$$

Note that for  $k \neq k_0$ , the term with  $q = k_0$  is now included in the summation. In the limit of large  $N$ , the term with  $A_{k_0,V}$  is in fact the *only* finite contribution to the whole sum, while all other terms vanish due to the factor  $1/N$ . Thus, using  $A_{k_0,V} = N(\tilde{\varepsilon}_{k_0} - \varepsilon_{k_0})$  from Eq. (17), we obtain a solution for  $\phi_{k,V}$  which reads as follows,

$$\phi_{k,V} = \arctan \left| \frac{\tilde{\varepsilon}_{k_0} - \varepsilon_{k_0}}{\tilde{\varepsilon}_{k_0} - \varepsilon_k} \right|. \quad (19)$$

As we will show below, the coefficient  $\phi_{k,V}$  will determine the amount of spectral weight which is transferred from the conduction band states to the bound state.

## 2.2 Spectral function

The bound state can for example be visualized by studying the spectral function, which is defined via the imaginary part of the one-particle Green's function,

$$\Im G(k, k, \omega) = \frac{1}{2\pi} \int_{-\infty}^{\infty} \langle [c_k^\dagger(-t), c_k]_+ \rangle e^{i\omega t} dt. \quad (20)$$

The time dependence and the expectation value are formed with the Hamiltonian  $\mathcal{H}_V$ . Correspondingly, the expectation value of an operator  $\mathcal{A}$  is defined as  $\langle \mathcal{A} \rangle = \text{Tr}(\mathcal{A} e^{-\beta \mathcal{H}_V})$ . Using the Mori-Zwanzig formalism [33, 34], the anticommutator correlation function can be rewritten to the form

$$\Im G(k, k, \omega) = \langle [c_k, \delta(\mathbf{L}_V - \omega) c_k^\dagger]_+ \rangle, \quad (21)$$

where  $\mathbf{L}_V \mathcal{A} = [\mathcal{H}_V, \mathcal{A}]$  is the Liouville operator. For occupied  $k$  states, the correlation function (21) can for example be measured by angle resolved photo emission (ARPES). Our method to calculate this quantity is by using the invariance of the trace under the transformation defined in Eqs. (2) and (3). This yields

$$\Im G(k, k, \omega) = \langle [\tilde{c}_{k,V}, \delta(\tilde{\mathbf{L}}_V - \omega) \tilde{c}_{k,V}^\dagger]_+ \rangle. \quad (22)$$

We evaluate this transformation according to the same method used for the Hamiltonian, i.e. through an expansion of  $\tilde{c}_{k,V}^\dagger = e^{X_V} c_k^\dagger e^{-X_V}$  in orders of  $X_V$  and stepwise calculation of the commutators using the expression for  $X_V$  from Eq. (4). The commutators are again calculated iteratively up to infinite order and summed up into sin- and cos-functions. In the case  $k \neq k_0$  we obtain

$$\tilde{c}_{k,V}^\dagger = \cos \phi_{k,V} c_k^\dagger + \sin \phi_{k,V} c_{k_0}^\dagger, \quad (23)$$

where  $\phi_{k,V}$  is the phase already introduced by Eq. (8). For the bound state  $k_0$  we find

$$\tilde{c}_{k_0,V}^\dagger = \left( \frac{1}{N} \sum_{k(\neq k_0)} \cos^2 \phi_{k,V} \right)^{1/2} c_{k_0}^\dagger + \frac{1}{\sqrt{N}} \sum_{k(\neq k_0)} \sin \phi_{k,V} c_k^\dagger, \quad (24)$$

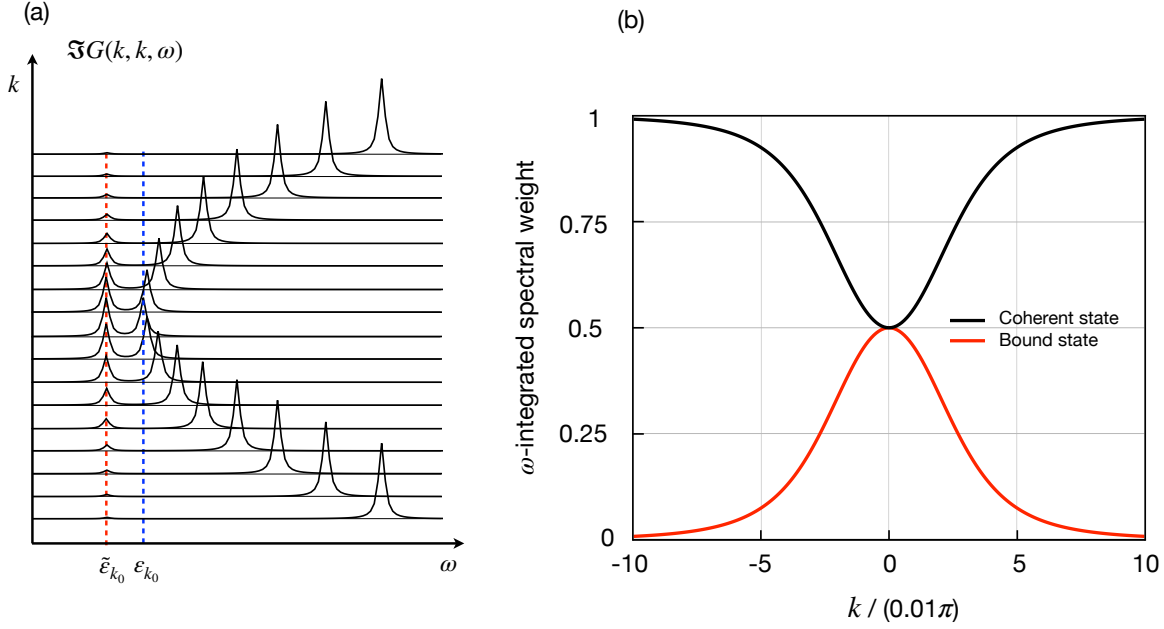


Figure 2: (a) One-particle Green's function for  $k \neq k_0$  of a non-magnetic impurity. The level broadening is introduced by hand and the broadening value is fixed to  $\eta = 0.1\tilde{\epsilon}_{k_0}$ . (b) Energy-integrated spectral weights  $\cos^2 \phi_{k,V}$  and  $\sin^2 \phi_{k,V}$  of the spectral function according to Eq. (25) where  $\phi_{k,V}$  is given by Eq. (19). The black line shows the coherent excitation and the red line shows the bound state excitation as a function of momentum  $k$ .

From Eqs. (23) and (24) one can immediately see that the anti-commutation relation for the transformed operator,  $[\tilde{c}_{k,V}^\dagger, \tilde{c}_{k,V}]_+ = 1$ , is fulfilled.

Inserting Eqs. (23) and (24) into the correlation function (22), we can directly evaluate the operator  $\delta(\tilde{\mathbf{L}}_V - \omega)$  by simply replacing the transformed Liouville operator  $\tilde{\mathbf{L}}_V$  with an eigenvalue of the corresponding one-particle operator it acts on. This is possible because it refers to the diagonalized Hamiltonian  $\tilde{\mathcal{H}}_V$ . Thus, we obtain for  $k \neq k_0$

$$\Im G(k, k, \omega) = \cos^2 \phi_{k,V} \delta(\epsilon_k - \omega) + \sin^2 \phi_{k,V} \delta(\tilde{\epsilon}_{k_0} - \omega), \quad (25)$$

and for  $k = k_0$

$$\Im G(k_0, k_0, \omega) = \frac{1}{N} \sum_{k(\neq k_0)} [\cos^2 \phi_{k,V} \delta(\tilde{\epsilon}_{k_0} - \omega) + \sin^2 \phi_{k,V} \delta(\epsilon_k - \omega)], \quad (26)$$

where in both cases the sum rule  $\int d\omega \Im G(k, k, \omega) = 1$  is fulfilled. We find the spectral function to exhibit a state at energy  $\tilde{\epsilon}_{k_0}$  in addition to the bare energies  $\epsilon_k$  of the free system. The energy  $\tilde{\epsilon}_{k_0}$  of this state is momentum-independent, indicating the state to be local in space – the hallmark of a bound state. Note that the intensity of the bound state (and also the other excitations) depends on the momentum  $k$ . This behavior is shown in Fig. 2(a) where the spectral function was calculated using Eq. (25) for a quadratic dispersion  $\epsilon_k$ . Furthermore, the spectral weights of the bound state and the dispersive states as calculated using the expression for the phase given by Eq. (19) is shown in Fig. 2(b). We find that the spectral weight of the bound state increases (at the cost of the dispersive states) if it comes closer to the conduction band.



### 3 Magnetic impurity in a superconductor

Our analytical approach to bound states in electron systems can readily be generalized to impurities in superconductors, including in particular magnetic impurities. Our starting point is a basic BCS-type  $s$ -wave superconductor coupled to a single magnetic impurity. Using a notation similar to Eq. 1 supplement by a spin index  $\sigma = \uparrow, \downarrow$ , this system is modelled by the Hamiltonian

$$\mathcal{H}_J = \underbrace{\sum_{\mathbf{k}\sigma} \varepsilon_{\mathbf{k}} c_{\mathbf{k}\sigma}^\dagger c_{\mathbf{k}\sigma}}_{=\mathcal{H}_0} + \Delta \sum_{\mathbf{k}} (c_{\mathbf{k}\uparrow}^\dagger c_{-\mathbf{k}\downarrow}^\dagger + c_{-\mathbf{k}\downarrow} c_{\mathbf{k}\uparrow}) + \underbrace{J \mathbf{S} \cdot \mathbf{s}_{\mathbf{r}_{\text{imp}}}}_{=\mathcal{H}_{1,J}}, \quad (27)$$

where  $\mathbf{S}$  and  $\mathbf{s}_{\mathbf{r}_{\text{imp}}}$  are the local impurity spin and the electron spin at the impurity site  $\mathbf{r}_{\text{imp}}$ , respectively. Before including the magnetic impurity, our approach requires to diagonalize the purely electronic Hamiltonian  $\mathcal{H}_0$ . This is achieved by introducing the usual Bogoliubov quasiparticles,

$$\alpha_{\mathbf{k}}^\dagger = u_{\mathbf{k}} c_{\mathbf{k}\uparrow}^\dagger - v_{\mathbf{k}} c_{-\mathbf{k}\downarrow}, \quad \beta_{\mathbf{k}}^\dagger = u_{\mathbf{k}} c_{-\mathbf{k}\downarrow}^\dagger + v_{\mathbf{k}} c_{\mathbf{k}\uparrow} \quad (28)$$

with

$$u_{\mathbf{k}}^2 = \frac{1}{2} \left( 1 + \frac{\varepsilon_{\mathbf{k}}}{\sqrt{\varepsilon_{\mathbf{k}}^2 + \Delta^2}} \right), \quad v_{\mathbf{k}}^2 = \frac{1}{2} \left( 1 - \frac{\varepsilon_{\mathbf{k}}}{\sqrt{\varepsilon_{\mathbf{k}}^2 + \Delta^2}} \right). \quad (29)$$

The electronic Hamiltonian  $\mathcal{H}_0$  is thus brought to the diagonal form

$$\mathcal{H}_0 = \sum_{\mathbf{k}} E_{\mathbf{k}} (\alpha_{\mathbf{k}}^\dagger \alpha_{\mathbf{k}} + \beta_{\mathbf{k}}^\dagger \beta_{\mathbf{k}}) + \sum_{\mathbf{k}} (\varepsilon_{\mathbf{k}} - E_{\mathbf{k}}), \quad (30)$$

with the quasiparticle energy  $E_{\mathbf{k}} = \sqrt{\varepsilon_{\mathbf{k}}^2 + \Delta^2}$ . Note that according to Sec. 2, the summation over  $\mathbf{k}$  includes possible bound state values  $\mathbf{k}_0$ . Placing the coordinate origin at the impurity site, the electron-impurity coupling reads

$$\mathcal{H}_{1,J} = \frac{J}{N} \sum_{\mathbf{k}\mathbf{k}'} \sum_{\alpha,\beta} \mathbf{S} \cdot \frac{\vec{\sigma}_{\alpha\beta}}{2} c_{\mathbf{k}\alpha}^\dagger c_{\mathbf{k}'\beta}. \quad (31)$$

Similar to the case of an impurity in a spinless electronic bath, the Hamiltonian  $\mathcal{H}_{1,J}$  can be diagonalized by a transformation generalizing Eq. (4). The precise form of this transformation depends on whether the impurity spin is considered in a classical approximation, or if its full quantum character is retained. As we discuss below, our approach is able to describe the key physics in both cases, in particular the presence of the Yu-Shiba-Rusinov (YSR) bound states [1–3].

#### 3.1 Classical spin

To describe a classical spin, the spin operator  $\mathbf{S}$  is replaced by a constant vector. We choose the spin to be oriented along  $z$  and thus set  $\mathbf{S} = S \mathbf{e}_z$  ( $\mathbf{e}_z$  being the unit vector along  $z$ ). The electron-impurity Hamiltonian then takes the form

$$\mathcal{H}_{1,Jcl} = \frac{JS}{2N} \sum_{\mathbf{k}\mathbf{k}'} [(u_{\mathbf{k}} v_{\mathbf{k}'} - u_{\mathbf{k}'} v_{\mathbf{k}}) (\alpha_{\mathbf{k}}^\dagger \beta_{\mathbf{k}'}^\dagger + \beta_{\mathbf{k}'} \alpha_{\mathbf{k}}) + (u_{\mathbf{k}} u_{\mathbf{k}'} + v_{\mathbf{k}'} v_{\mathbf{k}}) (\alpha_{\mathbf{k}}^\dagger \alpha_{\mathbf{k}'} - \beta_{\mathbf{k}}^\dagger \beta_{\mathbf{k}'})]. \quad (32)$$

Because a classical spin has no quantum fluctuations, the Hamiltonian is entirely quadratic in operators. The problem of a superconductor coupled to a classical spin can therefore again be solved by an exact mapping generalizing Eq. (2).

### 3.1.1 Exact solution of the scattering problem

We now proceed similar to Sec. 2, but with a modified unitary transformation. Comparing the Hamiltonians in Eqs. (32) and (1), we see that the problem is somewhat more involved because not all terms in Eq. (32) have the same sign. It will thus be convenient to decompose the full transformation into two steps. The first step brings the Hamiltonian to a form with symmetrized signs, while the second step diagonalizes the Hamiltonian.

*First transformation step*

For the generator of the unitary transformation in the first step, we make the ansatz

$$X_{Jcl} = \frac{\tilde{J}}{N} \sum_{\mathbf{k}\mathbf{k}'} \left[ \frac{u_{\mathbf{k}}v_{\mathbf{k}'} - u_{\mathbf{k}'}v_{\mathbf{k}}}{E_{\mathbf{k}} + E_{\mathbf{k}'}} (\alpha_{\mathbf{k}}^{\dagger}\beta_{\mathbf{k}'}^{\dagger} - \beta_{\mathbf{k}'}\alpha_{\mathbf{k}}) + \frac{u_{\mathbf{k}}u_{\mathbf{k}'} + v_{\mathbf{k}'}v_{\mathbf{k}}}{E_{\mathbf{k}} - E_{\mathbf{k}'}} (\alpha_{\mathbf{k}}^{\dagger}\alpha_{\mathbf{k}'} - \beta_{\mathbf{k}}^{\dagger}\beta_{\mathbf{k}'}) \right] \quad (33)$$

with an unknown coefficient  $\tilde{J}$ . Again, one sees that  $X_{Jcl}^{\dagger} = -X_{Jcl}$  is fulfilled. As before, we begin by calculating the term of first order in  $X_{Jcl}$  in the expansion of Eq. (5) for  $\mathcal{H}_0$ . Using the fact that  $\mathcal{H}_0$  is diagonal, we obtain

$$[X_{Jcl}, \mathcal{H}_0] = -\frac{\tilde{J}}{N} \sum_{\mathbf{k}\mathbf{k}'} \left[ (u_{\mathbf{k}}v_{\mathbf{k}'} - u_{\mathbf{k}'}v_{\mathbf{k}}) (\alpha_{\mathbf{k}}^{\dagger}\beta_{\mathbf{k}'}^{\dagger} + \beta_{\mathbf{k}'}\alpha_{\mathbf{k}}) + (u_{\mathbf{k}}u_{\mathbf{k}'} + v_{\mathbf{k}'}v_{\mathbf{k}}) (\alpha_{\mathbf{k}}^{\dagger}\alpha_{\mathbf{k}'} - \beta_{\mathbf{k}}^{\dagger}\beta_{\mathbf{k}'}) \right]. \quad (34)$$

As discussed in Sec. 2, the commutator with  $\mathcal{H}_{1,Jcl}$  leads to an internal momentum summation. We find

$$\begin{aligned} [X_{Jcl}, \mathcal{H}_{1,Jcl}] = & \\ & -\frac{JS}{2N} \tilde{J} \sum_{\mathbf{k}\mathbf{k}'} \left[ (u_{\mathbf{k}}u_{\mathbf{k}'} + v_{\mathbf{k}}v_{\mathbf{k}'}) (G_{\sigma\mathbf{k}} + G_{\sigma\mathbf{k}'}) + (u_{\mathbf{k}}v_{\mathbf{k}'} + u_{\mathbf{k}'}v_{\mathbf{k}}) (G_{\bar{\sigma}\mathbf{k}} + G_{\bar{\sigma}\mathbf{k}'}) \right] (\alpha_{\mathbf{k}}^{\dagger}\alpha_{\mathbf{k}'} + \beta_{\mathbf{k}}^{\dagger}\beta_{\mathbf{k}'}) \\ & -\frac{JS}{2N} \tilde{J} \sum_{\mathbf{k}\mathbf{k}'} \left[ (u_{\mathbf{k}}v_{\mathbf{k}'} - u_{\mathbf{k}'}v_{\mathbf{k}}) (G_{\sigma\mathbf{k}} - G_{\sigma\mathbf{k}'}) - (u_{\mathbf{k}}u_{\mathbf{k}'} - v_{\mathbf{k}}v_{\mathbf{k}'}) (G_{\bar{\sigma}\mathbf{k}} + G_{\bar{\sigma}\mathbf{k}'}) \right] (\alpha_{\mathbf{k}}^{\dagger}\beta_{\mathbf{k}'}^{\dagger} + \beta_{\mathbf{k}}\alpha_{\mathbf{k}'}), \end{aligned} \quad (35)$$

where we have introduced the abbreviations  $G_{\sigma(\bar{\sigma})\mathbf{k}} = \frac{1}{N} \sum_{\mathbf{q}} G_{\sigma(\bar{\sigma})}(\mathbf{q}, E_{\mathbf{k}})$  for the momentum summations of Green's functions in the superconducting state referring to the spin flip ' $\sigma$ ' and spin non-flip ' $\bar{\sigma}$ ' processes, respectively. The components of these matrix Green's functions are defined as

$$\begin{aligned} G_{\sigma}(\mathbf{q}, \omega) &= \langle [c_{\mathbf{q}\sigma}, \delta(\mathbf{L}_{Jcl} - \omega) c_{\mathbf{q}\sigma}^{\dagger}]_{+} \rangle = \frac{v_{\mathbf{q}}^2}{E_{\mathbf{q}} - \omega} - \frac{u_{\mathbf{q}}^2}{E_{\mathbf{q}} + \omega}, \\ G_{\bar{\sigma}}(\mathbf{q}, \omega) &= \langle [c_{\mathbf{q}\sigma}, \delta(\mathbf{L}_{Jcl} - \omega) c_{\mathbf{q}(-\sigma)}^{\dagger}]_{+} \rangle = u_{\mathbf{q}}v_{\mathbf{q}} \left( \frac{1}{E_{\mathbf{q}} - \omega} + \frac{1}{E_{\mathbf{q}} + \omega} \right). \end{aligned} \quad (36)$$

We now fix the coefficient  $\tilde{J}$  such that after the transformation, the first order of electron-impurity scattering is removed from the Hamiltonian. Comparing Eqs. (34) and (32), we find that this requires  $[X_{Jcl}, \mathcal{H}_0] = -\mathcal{H}_{1,Jcl}$ . Solving for  $\tilde{J}$ , this implies  $\tilde{J} = (JS)/2$ . At the same time, due to the presence of the non-vanishing commutator  $[X_{Jcl}, \mathcal{H}_{1,Jcl}]$ , the transformation generates an effective scattering of second order in  $J$ . All higher orders vanish in the thermodynamic limit: for a non-singular  $\tilde{J}$ , one finds along the lines of Sec. 2 that each higher order in the expansion

comes with an additional factor of  $1/\sqrt{N}$ . Using Eq. (35), the first step of our transformation is thus found to map the Hamiltonian to the form  $\tilde{\mathcal{H}}_{Jcl} = \mathcal{H}_0 + \tilde{\mathcal{H}}_{1,Jcl}$ , where the effective scattering  $\tilde{\mathcal{H}}_{1,Jcl}$  reads

$$\begin{aligned} \tilde{\mathcal{H}}_{1,Jcl} = & \\ & - \left(\frac{JS}{2}\right)^2 \frac{1}{N} \sum_{\mathbf{k}\mathbf{k}'} [(u_{\mathbf{k}}u_{\mathbf{k}'} + v_{\mathbf{k}}v_{\mathbf{k}'}) (G_{\sigma\mathbf{k}} + G_{\sigma\mathbf{k}'}) + (u_{\mathbf{k}}v_{\mathbf{k}'} + u_{\mathbf{k}'}v_{\mathbf{k}}) (G_{\bar{\sigma}\mathbf{k}} + G_{\bar{\sigma}\mathbf{k}'})] (\alpha_{\mathbf{k}}^\dagger \alpha_{\mathbf{k}'} + \beta_{\mathbf{k}}^\dagger \beta_{\mathbf{k}'}) \\ & - \left(\frac{JS}{2}\right)^2 \frac{1}{N} \sum_{\mathbf{k}\mathbf{k}'} [(u_{\mathbf{k}}v_{\mathbf{k}'} - u_{\mathbf{k}'}v_{\mathbf{k}}) (G_{\sigma\mathbf{k}} - G_{\sigma\mathbf{k}'}) - (u_{\mathbf{k}}u_{\mathbf{k}'} - v_{\mathbf{k}}v_{\mathbf{k}'}) (G_{\bar{\sigma}\mathbf{k}} + G_{\bar{\sigma}\mathbf{k}'})] (\alpha_{\mathbf{k}}^\dagger \beta_{\mathbf{k}'}^\dagger + \beta_{\mathbf{k}'} \alpha_{\mathbf{k}}). \end{aligned} \quad (37)$$

*Second transformation step*

As advertized before, the signs of all quasiparticle scattering terms are now identical. As a result, we can next apply a second transformation similar to the one used in Sec. 2 to eliminate the non-diagonal terms. The generator used in this transformation of course has to be tailored towards the Hamiltonian  $\tilde{\mathcal{H}}_{1,Jcl}$  in Eq. (37), and we thus use the ansatz

$$\begin{aligned} \tilde{X}_{Jcl} = & \\ & - \frac{1}{N} \sum_{\mathbf{k}\mathbf{k}'} \frac{A_{\mathbf{k},Jcl} + A_{\mathbf{k}',Jcl}}{E_{\mathbf{k}} - E_{\mathbf{k}'}} (u_{\mathbf{k}}u_{\mathbf{k}'} + v_{\mathbf{k}}v_{\mathbf{k}'} + u_{\mathbf{k}}v_{\mathbf{k}'} + u_{\mathbf{k}'}v_{\mathbf{k}}) (\alpha_{\mathbf{k}}^\dagger \alpha_{\mathbf{k}'} + \beta_{\mathbf{k}}^\dagger \beta_{\mathbf{k}'}) \\ & - \frac{1}{N} \sum_{\mathbf{k}\mathbf{k}'} \left[ (u_{\mathbf{k}}v_{\mathbf{k}'} - u_{\mathbf{k}'}v_{\mathbf{k}}) \frac{A_{\mathbf{k},Jcl} - A_{\mathbf{k}',Jcl}}{E_{\mathbf{k}} + E_{\mathbf{k}'}} - (u_{\mathbf{k}}u_{\mathbf{k}'} - v_{\mathbf{k}}v_{\mathbf{k}'}) \frac{A_{\mathbf{k},Jcl} + A_{\mathbf{k}',Jcl}}{E_{\mathbf{k}} + E_{\mathbf{k}'}} \right] (\alpha_{\mathbf{k}}^\dagger \beta_{\mathbf{k}'}^\dagger - \beta_{\mathbf{k}'} \alpha_{\mathbf{k}}), \end{aligned} \quad (38)$$

where we have introduced unknown coefficients  $A_{\mathbf{k},Jcl}$  in analogy to the way of constructing the generator  $X_V$  in Eq. (4). Note that a possible bound state is again included in the momentum summations.

Next, we calculate the commutator of  $\tilde{X}_{Jcl}$  and  $\tilde{\mathcal{H}}_{1,Jcl}$ . The result has the same form as  $\tilde{\mathcal{H}}_{1,Jcl}$  given by Eq. (37), but with products of Green's function components and the unknown coefficients as prefactors to the Bogoliubov coefficients. Concretely, we obtain

$$\begin{aligned} [\tilde{X}_{Jcl}, \tilde{\mathcal{H}}_{1,Jcl}] = & \left(\frac{JS}{2}\right)^2 \frac{1}{N} \sum_{\mathbf{k}\mathbf{k}'} (G_{\sigma\mathbf{k}} + G_{\bar{\sigma}\mathbf{k}}) (G_{\sigma\mathbf{k}'} + G_{\bar{\sigma}\mathbf{k}'}) \\ & \times (u_{\mathbf{k}}u_{\mathbf{k}'} + v_{\mathbf{k}}v_{\mathbf{k}'} + u_{\mathbf{k}}v_{\mathbf{k}'} + u_{\mathbf{k}'}v_{\mathbf{k}}) (A_{\mathbf{k},Jcl} + A_{\mathbf{k}',Jcl}) (\alpha_{\mathbf{k}}^\dagger \alpha_{\mathbf{k}'} + \beta_{\mathbf{k}}^\dagger \beta_{\mathbf{k}'}) \\ & + \left(\frac{JS}{2}\right)^2 \frac{1}{N} \sum_{\mathbf{k}\mathbf{k}'} (G_{\sigma\mathbf{k}} + G_{\bar{\sigma}\mathbf{k}}) (G_{\sigma\mathbf{k}'} - G_{\bar{\sigma}\mathbf{k}'}) [(u_{\mathbf{k}}u_{\mathbf{k}'} - v_{\mathbf{k}}v_{\mathbf{k}'}) (A_{\mathbf{k},Jcl} + A_{\mathbf{k}',Jcl}) \\ & - (u_{\mathbf{k}}v_{\mathbf{k}'} - u_{\mathbf{k}'}v_{\mathbf{k}}) (A_{\mathbf{k},Jcl} - A_{\mathbf{k}',Jcl})] (\alpha_{\mathbf{k}}^\dagger \beta_{\mathbf{k}'}^\dagger + \beta_{\mathbf{k}'} \alpha_{\mathbf{k}}). \end{aligned} \quad (39)$$

Compared to the effective scattering Hamiltonian (37), the operator structure and the structure of the coherence factors is fully maintained. All higher order contributions can be summarized to sin- and cos-functions. They appear as prefactors, and therefore do not change the algebraic structure of Eq. (39).

As in Sec. 2, we numerically solve for the coefficients  $A_{\mathbf{k},Jcl}$  such that the Hamiltonian becomes  $\mathbf{k}$ -diagonal. Generally speaking, we obtain a very similar result to the case of a potential impurity in a spinless electron system: some coefficients  $A_{\mathbf{k},Jcl}$  can become singular, and this indicates

the formation of bound states. Let us again illustrate this result for the case of a single magnetic impurity, for which our numerics indicate that there is a bound state, and for which one of the coefficients  $A_{\mathbf{k},Jcl}$  diverges. As before, we call the corresponding quantum number  $\mathbf{k}_0$ . The yet unknown singular coefficient  $A_{\mathbf{k}_0,Jcl}$  is again determined by the condition that the final Hamiltonian is diagonal in  $\mathbf{k}$ . Our numerics shows that the state associated with  $\mathbf{k}_0$  is located at the (normal state) Fermi surface where the Bogoliubov coefficients have equal values  $u_{\mathbf{k}} = v_{\mathbf{k}} = 1/\sqrt{2}$ . We therefore focus our discussion on quantum numbers  $\mathbf{k}$  and  $\mathbf{k}'$  near the Fermi surface, for which we find  $G_{\sigma(\bar{\sigma})\mathbf{k}} = G_{\sigma(\bar{\sigma})\mathbf{k}'}$ , and where the expressions for  $\tilde{\mathcal{H}}_{1,Jcl}$  and  $[\tilde{X}_{Jcl}, \tilde{\mathcal{H}}_{1,Jcl}]$  from Eqs. (37) and (39) simplify to

$$\begin{aligned} \tilde{\mathcal{H}}_{1,Jcl} \Big|_{|\mathbf{k}|,|\mathbf{k}'| \approx k_F} &= -\left(\frac{JS}{2}\right)^2 \frac{1}{N} \sum_{\mathbf{k}\mathbf{k}'} (G_{\sigma\mathbf{k}} + G_{\bar{\sigma}\mathbf{k}}) (\alpha_{\mathbf{k}}^\dagger \alpha_{\mathbf{k}'} + \beta_{\mathbf{k}}^\dagger \beta_{\mathbf{k}'} + \text{h.c.}) \\ [\tilde{X}_{Jcl}, \tilde{\mathcal{H}}_{1,Jcl}] \Big|_{|\mathbf{k}|,|\mathbf{k}'| \approx k_F} &= \frac{(JS)^2}{2} \frac{1}{N} \sum_{\mathbf{k}\mathbf{k}'} (G_{\sigma\mathbf{k}} + G_{\bar{\sigma}\mathbf{k}})^2 A_{\mathbf{k},Jcl} (\alpha_{\mathbf{k}}^\dagger \alpha_{\mathbf{k}'} + \beta_{\mathbf{k}}^\dagger \beta_{\mathbf{k}'} + \text{h.c.}). \end{aligned} \quad (40)$$

The form of the effective scattering  $[\tilde{X}_{Jcl}, \tilde{\mathcal{H}}_{1,Jcl}]$  is thus found to be very similar to Eq. (6). A self-consistent solution for the transformation coefficient  $A_{\mathbf{k}_0,Jcl}$  at the singular point  $\mathbf{k}_0$  can therefore be found similar to the treatment of Eq. (11). Comparing Eqs. (40) with the corresponding expressions in the non-magnetic case, Eqs. (1) and (6), one finds that the replacements  $V/2 \rightarrow -\left(\frac{JS}{2}\right)^2 (G_{\sigma\mathbf{k}_0} + G_{\bar{\sigma}\mathbf{k}_0})$  in the numerator and  $\frac{V}{N} \sum_{q(\neq k_0)} \frac{1}{\bar{\epsilon}_{k_0} - \bar{\epsilon}_q} \rightarrow \frac{(JS)^2}{2} (G_{\sigma\mathbf{k}_0} + G_{\bar{\sigma}\mathbf{k}_0})^2$  in the denominator of Eq. (11) can be used to immediately obtain a solution for the transformation coefficient also in the present case. With these replacements we find

$$A_{\mathbf{k}_0,Jcl} = \frac{-\left(\frac{JS}{2}\right)^2 (G_{\sigma\mathbf{k}_0} + G_{\bar{\sigma}\mathbf{k}_0})}{1 - \left(\frac{JS}{2}\right)^2 (G_{\sigma\mathbf{k}_0} + G_{\bar{\sigma}\mathbf{k}_0})^2}, \quad (41)$$

with  $G_{\sigma(\bar{\sigma})\mathbf{k}_0} = \frac{1}{N} \sum_{\mathbf{q}} G_{\sigma(\bar{\sigma})}(\mathbf{q}, \omega_0)$ . This expression becomes singular if the energy  $\omega_0$  fulfills the equation

$$\frac{JS}{2N} \sum_{\mathbf{q}} [G_{\sigma}(\mathbf{q}, \omega_0) + G_{\bar{\sigma}}(\mathbf{q}, \omega_0)] = 1. \quad (42)$$

According to our above discussion, the solution  $\omega_0$  for which Eq. (42) is fulfilled has to be interpreted as the energy of a bound state. To explicitly calculate  $\omega_0$ , we use the expressions of the Green's functions in Eq. (36), of the Bogoliubov coefficients in Eq. (29), and of the BCS density of states,

$$\nu(E) = \nu_0 \Theta(|E| - \Delta) \frac{|E|}{\sqrt{E^2 - \Delta^2}}, \quad (43)$$

where  $\nu_0$  is the density of states at the Fermi level in the normal state. We also express the momentum summation in terms of an energy integration and calculate the corresponding integral analytically. The result is

$$\frac{1}{N} \sum_{\mathbf{q}} [G_{\sigma}(\mathbf{q}, \omega_0) + G_{\bar{\sigma}}(\mathbf{q}, \omega_0)] = \nu_0 \pi \frac{\Delta + \omega_0}{\sqrt{\Delta^2 - \omega_0^2}}. \quad (44)$$

Thus, the energy of the bound state is given by the solution of the equation

$$1 - \frac{JS}{2} \nu_0 \pi \frac{\Delta + \omega_0}{\sqrt{\Delta^2 - \omega_0^2}} = 0. \quad (45)$$

This equation has a solution for  $\omega_0$  only in the superconducting state, i.e. if  $\Delta \neq 0$ . In this case its positive solution is

$$\omega_0 = \Delta \frac{1 - \left(\frac{JS\nu_0\pi}{2}\right)^2}{1 + \left(\frac{JS\nu_0\pi}{2}\right)^2}, \quad (46)$$

which exactly agrees with the original result obtained by Shiba [2]. Thus, our bound state has to be identified with the well-known YSR state appearing in the spectral function as a pair of peaks inside the superconducting gap.

### 3.1.2 Spectral function

To visualize the YSR state, we again consider a one-particle spectral function similar to Eq. (22). For the sake of concreteness, let us focus on the spin-up spectral density defined as

$$\Im G(\mathbf{k}, \mathbf{k}, \omega) = \langle [\tilde{c}_{\mathbf{k}\uparrow, Jcl}, \delta(\tilde{L}_{Jcl} - \omega)\tilde{c}_{\mathbf{k}\uparrow, Jcl}^\dagger]_+ \rangle. \quad (47)$$

We evaluate the Liouville operator and the expectation value by replacing the electron operators with the Bogoliubov quasiparticles using Eq. (28) and obtain

$$\Im G(\mathbf{k}, \mathbf{k}, \omega) = \langle [u_{\mathbf{k}}\tilde{\alpha}_{\mathbf{k}, Jcl} + v_{\mathbf{k}}\tilde{\beta}_{\mathbf{k}, Jcl}^\dagger, \delta(\tilde{L}_{Jcl} - \omega)(u_{\mathbf{k}}\tilde{\alpha}_{\mathbf{k}, Jcl}^\dagger + v_{\mathbf{k}}\tilde{\beta}_{\mathbf{k}, Jcl})]_+ \rangle. \quad (48)$$

Similar to the discussion of Sec. 2, the transformed quasiparticle operators are calculated by applying the same transformations as we did for the Hamiltonian. We find for  $\mathbf{k} \neq \mathbf{k}_0$

$$\begin{aligned} \tilde{\alpha}_{\mathbf{k}, Jcl}^\dagger &= \cos \phi_{\mathbf{k}, Jcl} \alpha_{\mathbf{k}}^\dagger - \sin \phi_{\mathbf{k}, Jcl} \left[ \frac{u_{\mathbf{k}} + v_{\mathbf{k}}}{\sqrt{2}} \alpha_{\mathbf{k}_0}^\dagger + \frac{u_{\mathbf{k}} - v_{\mathbf{k}}}{\sqrt{2}} \beta_{\mathbf{k}_0} \right], \\ \tilde{\beta}_{\mathbf{k}, Jcl}^\dagger &= \cos \phi_{\mathbf{k}, Jcl} \beta_{\mathbf{k}}^\dagger - \sin \phi_{\mathbf{k}, Jcl} \left[ \frac{u_{\mathbf{k}} + v_{\mathbf{k}}}{\sqrt{2}} \beta_{\mathbf{k}_0}^\dagger - \frac{u_{\mathbf{k}} - v_{\mathbf{k}}}{\sqrt{2}} \alpha_{\mathbf{k}_0} \right], \end{aligned} \quad (49)$$

where the momentum-dependent phase coefficient  $\phi_{\mathbf{k}, Jcl}$  in the superconducting state  $\Delta \neq 0$  is given by

$$\phi_{\mathbf{k}, Jcl} = \arctan \left| \frac{\omega_0 - \Delta}{\omega_0 - E_{\mathbf{k}}} \right|. \quad (50)$$

Note that Eqs. (46) and (50) imply that  $\phi_{\mathbf{k}, Jcl}$  is zero in the normal state, which in turn means that the bound state discussed here disappears in that limit. Inserting expressions (49) in Eq. (48) we obtain for the spectral function at  $\mathbf{k} \neq \mathbf{k}_0$

$$\begin{aligned} \Im G(\mathbf{k}, \mathbf{k}, \omega) &= \frac{1}{2} \cos^2 \phi_{\mathbf{k}, Jcl} \left[ \left(1 + \frac{\varepsilon_{\mathbf{k}}}{E_{\mathbf{k}}}\right) \delta(E_{\mathbf{k}} - \omega) + \left(1 - \frac{\varepsilon_{\mathbf{k}}}{E_{\mathbf{k}}}\right) \delta(-E_{\mathbf{k}} - \omega) \right] \\ &+ \frac{1}{2} \sin^2 \phi_{\mathbf{k}, Jcl} [\delta(\omega_0 - \omega) + \delta(-\omega_0 - \omega)], \end{aligned} \quad (51)$$

and at  $\mathbf{k} = \mathbf{k}_0$

$$\begin{aligned} \Im G(\mathbf{k}_0, \mathbf{k}_0, \omega) &= \frac{1}{2N} \sum_{\mathbf{k}} \left\{ \cos^2 \phi_{\mathbf{k}, Jcl} [\delta(\omega_0 - \omega) + \delta(-\omega_0 - \omega)] \right. \\ &\left. + \sin^2 \phi_{\mathbf{k}, Jcl} \left[ \left(1 + \frac{\varepsilon_{\mathbf{k}}}{E_{\mathbf{k}}}\right) \delta(E_{\mathbf{k}} - \omega) + \left(1 - \frac{\varepsilon_{\mathbf{k}}}{E_{\mathbf{k}}}\right) \delta(-E_{\mathbf{k}} - \omega) \right] \right\}, \end{aligned} \quad (52)$$

where the bound state energy is given by Eq. (46). In the following, let us focus on the spectral function at  $\mathbf{k} \neq \mathbf{k}_0$ . In addition to the usual dispersive states (first line of Eq. (51)), there appears in the second line a pair of bound states. Those have the momentum-independent energy  $\pm\omega_0$  above and below the Fermi level, but inside the superconducting gap. Note that the sum rule  $\int d\omega \Im G(\mathbf{k}, \mathbf{k}, \omega) = 1$  is fulfilled.

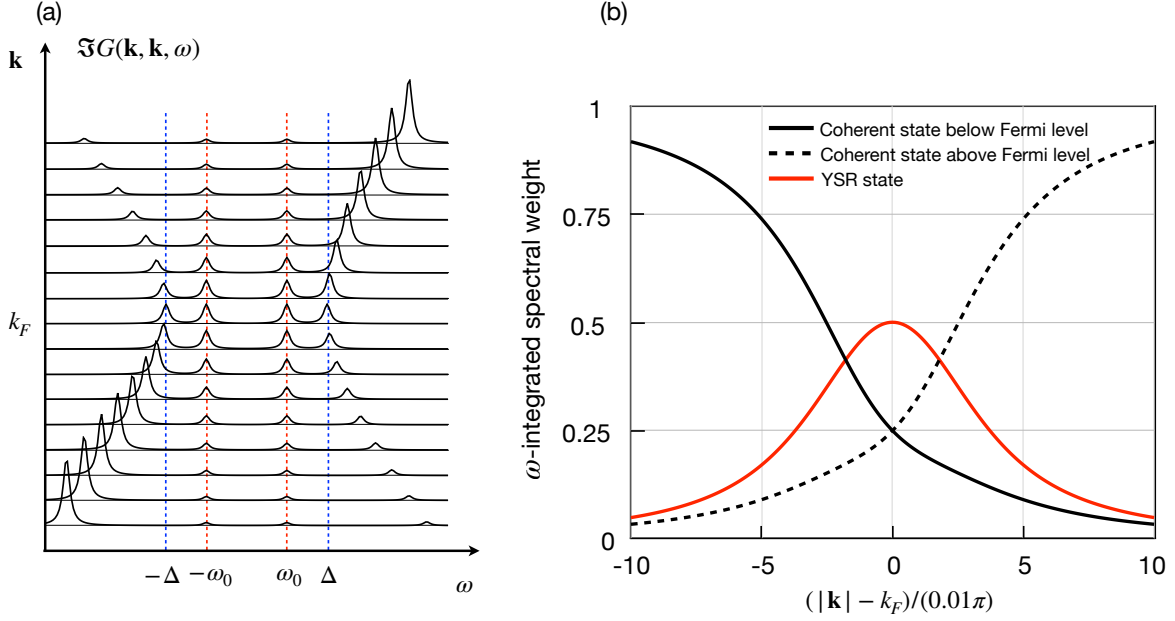


Figure 3: (a) One-particle Green's function for a classical spin in a momentum region  $\mathbf{k} \neq \mathbf{k}_0$  near the Fermi surface. The chosen parameters are  $J = \Delta = 0.004W$ ,  $\omega_0 = 0.002W$ , and  $S = 1/2$  ( $W$ : band width). The level broadening is fixed to the value  $\eta = 2 \cdot 10^{-4}W$ . (b) Energy-integrated spectral weight of the different excitations in the spectral function of panel (a) as a function of momentum.

The behavior of the YSR state in the spectral function is visualized in Fig. 3(a) where the spectral function from Eq. (51) is calculated explicitly for a specific set of parameters, and for a number of momenta  $\mathbf{k} \neq \mathbf{k}_0$ . One finds the typical dispersionless double-peak structure of the YSR state inside the superconducting gap where the intensity is strongest in the vicinity of the gap edge. Furthermore, one clearly recognizes the two distinct branches of the superconducting quasiparticles below and above the Fermi level. The spectral weight of the corresponding excitations which are shown in Fig. 3(b) reveals an intensity maximum of the YSR state near the Fermi momentum of the normal state. The momentum dependence of the coherent excitation intensity, however, is mainly influenced by the Bogoliubov coefficients  $|u_{\mathbf{k}}|^2$  and  $|v_{\mathbf{k}}|^2$ .

### 3.2 Quantum spin

Unlike the case of a classical spin in a superconductor, or the even simpler case of a potential impurity in a spinless electron bath, the case of a quantum spin immersed into an  $s$ -wave superconductor constitutes an interacting quantum problem, and therefore cannot be solved exactly. Our approach can nevertheless be generalized to take this interaction into account on an approximate level. Our approximation scheme has already been shown to successfully describe the Kondo

effect of a quantum spin coupled to a normal-state electron system [37], and it can therefore be expected to also yields excellent results when applied to a superconducting system. After discussing technical details of the transformation we use to tackle the problem, we will first compare our results with recent experimental and numerical studies, and then show new original results of the momentum-resolved spectral function. We furthermore discuss that our approach clearly illustrates how a Kondo singlet with an energy scale  $k_B T_K$  (with  $k_B$  being the Boltzmann constant and  $T_K$  the Kondo temperature) competes with the singlet state of the superconductor leading to a transition from an unscreened, free-spin ground state to a Kondo-screened state [35].

### 3.2.1 Approximate solution of the scattering problem

We consider the case of a single local magnetic impurity represented by a quantum spin of arbitrary size that is described by an angular momentum operator  $\mathbf{S}$ . This impurity is coupled to the electrons in an  $s$ -wave BCS superconductor, and the coordinate origin is again chosen to coincide with the impurity position. Replacing the conduction electron operators with the ones of Bogoliubov quasiparticles using Eq. (28), and introducing the shorthands  $C_1^\pm = u_{\mathbf{k}}u_{\mathbf{k}'} \pm v_{\mathbf{k}}v_{\mathbf{k}'}$ ,  $C_2^\pm = u_{\mathbf{k}}v_{\mathbf{k}'} \pm v_{\mathbf{k}}u_{\mathbf{k}'}$  for combinations of Bogoliubov coefficients, the electron-impurity-coupling takes the form

$$\begin{aligned} \mathcal{H}_{1,J} = & \frac{J}{2N} \sum_{\mathbf{k}\mathbf{k}'} \left\{ C_1^+ \left( \alpha_{\mathbf{k}}^\dagger \alpha_{\mathbf{k}'} S_z - \beta_{\mathbf{k}}^\dagger \beta_{\mathbf{k}'} S_z + \alpha_{\mathbf{k}}^\dagger \beta_{\mathbf{k}'} S^- + \beta_{\mathbf{k}}^\dagger \alpha_{\mathbf{k}'} S^+ \right) \right. \\ & \left. + C_2^- \left[ \left( \alpha_{\mathbf{k}}^\dagger \beta_{\mathbf{k}'}^\dagger + \beta_{\mathbf{k}'} \alpha_{\mathbf{k}} \right) S_z + \frac{1}{2} \left( \beta_{\mathbf{k}'} \beta_{\mathbf{k}} - \alpha_{\mathbf{k}}^\dagger \alpha_{\mathbf{k}'}^\dagger \right) S^- + \frac{1}{2} \left( \beta_{\mathbf{k}}^\dagger \beta_{\mathbf{k}'}^\dagger - \alpha_{\mathbf{k}'} \alpha_{\mathbf{k}} \right) S^+ \right] \right\}. \end{aligned} \quad (53)$$

Here,  $S^+$  ( $S^-$ ) is the spin raising (lowering) operator, while  $S_z$  denotes the  $z$ -component of the spin operator  $\mathbf{S}$ . At this point, all we demand of these operators is that they satisfy the commutation relations  $[S^+, S^-] = 2S_z$ ,  $[S_z, S^-] = -S^-$ , and  $[S_z, S^+] = S^+$ . For the rest of the paper we keep the simplified notation for  $C_1^\pm$  and  $C_2^\pm$  but emphasize that these coefficients are momentum dependent and always meant to refer to the momentum vectors  $\mathbf{k}$  and  $\mathbf{k}'$  according to the above definition.

To solve the scattering problem, we apply a two-step procedure similar to the case of a classical spin described in Sec. 3.1 that first brings the transformed Hamiltonian to a form with symmetrized signs, and then diagonalizes the Hamiltonian by eliminating the remaining couplings between states with different  $\mathbf{k}$ .

#### First transformation step

For the first step, we use an ansatz similar to Eq. (33), namely

$$\begin{aligned} X_J = & \frac{1}{N} \sum_{\mathbf{k}\mathbf{k}'} \frac{\tilde{J}_{\mathbf{k}} + \tilde{J}_{\mathbf{k}'}}{2} \left\{ \frac{C_1^+}{E_{\mathbf{k}} - E_{\mathbf{k}'}} \left( \alpha_{\mathbf{k}}^\dagger \alpha_{\mathbf{k}'} S_z - \beta_{\mathbf{k}}^\dagger \beta_{\mathbf{k}'} S_z + \alpha_{\mathbf{k}}^\dagger \beta_{\mathbf{k}'} S^- + \beta_{\mathbf{k}}^\dagger \alpha_{\mathbf{k}'} S^+ \right) \right. \\ & \left. + \frac{C_2^-}{E_{\mathbf{k}} + E_{\mathbf{k}'}} \left[ \left( \alpha_{\mathbf{k}}^\dagger \beta_{\mathbf{k}'}^\dagger - \beta_{\mathbf{k}'} \alpha_{\mathbf{k}} \right) S_z - \frac{1}{2} \left( \beta_{\mathbf{k}'} \beta_{\mathbf{k}} + \alpha_{\mathbf{k}}^\dagger \alpha_{\mathbf{k}'}^\dagger \right) S^- + \frac{1}{2} \left( \beta_{\mathbf{k}}^\dagger \beta_{\mathbf{k}'}^\dagger + \alpha_{\mathbf{k}'} \alpha_{\mathbf{k}} \right) S^+ \right] \right\}. \end{aligned} \quad (54)$$

The yet unknown coefficients  $\tilde{J}_{\mathbf{k}}$  replacing the coefficient  $\tilde{J}$  in Eq. (33) will take the role of effectively renormalized exchange couplings. They are determined by the condition that all terms having the operator structure of  $\mathcal{H}_{1,J}$  are eliminated within the first transformation step. At the same time, the transformed Hamiltonian

$$\tilde{\mathcal{H}}_J = e^{X_J} \mathcal{H} e^{-X_J} = \mathcal{H}_0 + \tilde{\mathcal{H}}_{1,J} \quad (55)$$

resulting from this first step will generate a new scattering term  $\tilde{\mathcal{H}}_{1,J}$  that has to be eliminated in the second transformation step.

Using the ansatz of  $X_J$  given by Eq. (54), we first evaluate the unitary transformation  $e^{X_J} \mathcal{H}_J e^{-X_J}$ . As in the case of a classical spin, the lowest order generates new contributions to an effective electron-impurity scattering. Since the spin is now a quantum operator, however, these new terms are qualitatively different from the classical case because they are composed of terms that are not quadratic in operators. We distinguish two types of terms,

$$[X_J, \mathcal{H}_{1,J}] = [X_J, \mathcal{H}_{1,J}]_1 + [X_J, \mathcal{H}_{1,J}]_2 \quad (56)$$

$$\begin{aligned} [X_J, \mathcal{H}_{1,J}]_1 &= \frac{J}{2N^2} \sum_{\mathbf{k}\mathbf{k}'} \sum_{k_1 k_1'} \frac{\tilde{J}_{\mathbf{k}} + \tilde{J}_{\mathbf{k}'}}{E_{\mathbf{k}} - E_{\mathbf{k}'}} (u_{\mathbf{k}} u_{\mathbf{k}'} + v_{\mathbf{k}} v_{\mathbf{k}'}) \\ &\quad \times (u_{k_1} u_{k_1'} + v_{k_1} v_{k_1'}) \left\{ [\alpha_{\mathbf{k}}^\dagger \alpha_{\mathbf{k}'}, \alpha_{k_1}^\dagger \alpha_{k_1'}] (\vec{S} \cdot \vec{S}) + (\dots) (\vec{S} \cdot \vec{S}) \right\}, \end{aligned} \quad (57)$$

$$\begin{aligned} [X_J, \mathcal{H}_{1,J}]_2 &= \frac{J}{2N^2} \sum_{\mathbf{k}\mathbf{k}'} \sum_{k_1 k_1'} \frac{\tilde{J}_{\mathbf{k}} + \tilde{J}_{\mathbf{k}'}}{E_{\mathbf{k}} - E_{\mathbf{k}'}} (u_{\mathbf{k}} u_{\mathbf{k}'} + v_{\mathbf{k}} v_{\mathbf{k}'}) \\ &\quad \times (u_{k_1} u_{k_1'} + v_{k_1} v_{k_1'}) \left\{ \alpha_{\mathbf{k}}^\dagger \beta_{\mathbf{k}'} \beta_{k_1'}^\dagger \alpha_{k_1} [S^-, S^+] + (\dots) [S^-, S^+] \right\}. \end{aligned} \quad (58)$$

where the dots (...) indicate the existence of further terms of the same operator structure. The terms generated by  $[X_J, \mathcal{H}_{1,J}]_1$  are quadratic in the fermionic operators. In addition, the scalar product of quantum spin operators ( $\vec{S} \cdot \vec{S}$ ) can immediately be replaced with the number  $S(S+1)$  because the Hamiltonian is rotational invariant and therefore this product is conserved. This yields

$$\begin{aligned} [X_J, \mathcal{H}_{1,J}]_1 &= -\frac{J}{2} S(S+1) \frac{1}{N} \sum_{\mathbf{k}\mathbf{k}'} \left\{ [C_1^+(\mathcal{J}_{\sigma\mathbf{k}} + \mathcal{J}_{\sigma\mathbf{k}'}) + C_2^+(\mathcal{J}_{\bar{\sigma}\mathbf{k}} + \mathcal{J}_{\bar{\sigma}\mathbf{k}'})] (\alpha_{\mathbf{k}}^\dagger \alpha_{\mathbf{k}'} + \beta_{\mathbf{k}}^\dagger \beta_{\mathbf{k}'}) \right. \\ &\quad \left. - [C_2^-(\mathcal{J}_{\sigma\mathbf{k}} - \mathcal{J}_{\sigma\mathbf{k}'}) - C_1^-(\mathcal{J}_{\bar{\sigma}\mathbf{k}} + \mathcal{J}_{\bar{\sigma}\mathbf{k}'})] (\alpha_{\mathbf{k}}^\dagger \beta_{\mathbf{k}'}^\dagger + \beta_{\mathbf{k}'} \alpha_{\mathbf{k}}) \right\}, \end{aligned} \quad (59)$$

where we introduced the short-hand notation

$$\mathcal{J}_{\sigma\mathbf{k}} = \frac{1}{N} \sum_{\mathbf{q}} (\tilde{J}_{\mathbf{k}} + \tilde{J}_{\mathbf{q}}) G_{\sigma}(\mathbf{q}, E_{\mathbf{k}}). \quad (60)$$

The corresponding equation for  $\mathcal{J}_{\bar{\sigma}\mathbf{k}}$  is obtained by the replacement  $\sigma \rightarrow \bar{\sigma}$ . Eq. (59) is a direct generalization of Eq. (35). The effective scattering generated from  $[X_J, \mathcal{H}_{1,J}]_1$  hence has the same form as  $\tilde{\mathcal{H}}_{1,Jcl}$  given by Eq. (37), but with modified prefactors. It can be treated as in the case of a classical spin by a second unitary transformation. This is done further below.

In contrast, the terms generated by  $[X_J, \mathcal{H}_{1,J}]_2$  describe a true many-body interaction that only arises in the case of a quantum spin. In the following, we show that these terms can be approximately brought to the operator form of the original interaction  $\mathcal{H}_{1,J}$ . This allows us to fix the coefficients  $\tilde{J}_{\mathbf{k}}$  such that, similar to the classical spin case, only quadratic scattering terms of the form of Eq. (57) remain after the first transformation (55). The corresponding renormalization equation for  $\tilde{J}_{\mathbf{k}}$  is solved numerically.

To find this renormalization equation, we have to compare the scattering interaction resulting from the lowest order of the first transformation, see Eq. (58), with the original scattering  $\mathcal{H}_{1,J}$  of Eq. (53). It is at this step that our method requires an approximation to be made. Namely, we apply a factorization approximation [31] which replaces a pair of fermionic operators with



a corresponding expectation value. The procedure of the factorization is carried out as follows. Each time a transformation yields a term with four Bogoliubov quasiparticle operators of the form  $\alpha^\dagger \alpha \beta^\dagger \beta$ , we make the approximation

$$\alpha^\dagger \alpha \beta^\dagger \beta \approx \alpha^\dagger \alpha \langle \beta^\dagger \beta \rangle + \langle \alpha^\dagger \alpha \rangle \beta^\dagger \beta - \langle \alpha^\dagger \alpha \rangle \langle \beta^\dagger \beta \rangle.$$

A similar replacement is done for terms with four Bogoliubov operators of the same type ( $\alpha^\dagger$  or  $\beta^\dagger$ ) by taking into account normal ordering. The factorization restores an operator structure that is quadratic in fermionic operators, and therefore allows us to derive a renormalization equation for  $\tilde{J}_k$ . The price to pay is that these renormalization equations contain expectation values that have to be calculated self-consistently.

The above factorization approximation looks somewhat similar to a mean field approximation. However, it differs from such a treatment since the factorization is applied at each order of the unitary transformation. The resulting series is summed up to infinite order since all orders have a similar structure. Our approach is thus different from a simple mean field approximation in which a single factorization is applied. As discussed in Ref. [37], our factorization approach has already been employed successfully for a treatment of the Kondo effect in a normal-state metal, which illustrates its non-perturbative power.

Applying the factorization approximation to  $[X_J, \mathcal{H}_{1,J}]_2$ , we obtain

$$\begin{aligned} [X_J, \mathcal{H}_{1,J}]_{2,\text{factorized}} &= \frac{J}{2N} \sum_{\mathbf{k}\mathbf{k}'} \left\{ \left[ C_1^+(B_{\sigma\mathbf{k}} + B_{\sigma\mathbf{k}'}) - C_2^+(B_{\bar{\sigma}\mathbf{k}} + B_{\bar{\sigma}\mathbf{k}'}) \right] \right. \\ &\times \left[ \alpha_{\mathbf{k}}^\dagger \alpha_{\mathbf{k}'} S_z - \beta_{\mathbf{k}}^\dagger \beta_{\mathbf{k}'} S_z + \alpha_{\mathbf{k}}^\dagger \beta_{\mathbf{k}'} S^- + \beta_{\mathbf{k}}^\dagger \alpha_{\mathbf{k}} S^+ \right] \\ &+ \left[ C_2^-(B_{\sigma\mathbf{k}} + B_{\sigma\mathbf{k}'}) + C_1^-(B_{\bar{\sigma}\mathbf{k}} - B_{\bar{\sigma}\mathbf{k}'}) \right] \left[ (\alpha_{\mathbf{k}}^\dagger \beta_{\mathbf{k}'}^\dagger + \beta_{\mathbf{k}'} \alpha_{\mathbf{k}}) S_z \right. \\ &\left. \left. + \frac{1}{2} (\beta_{\mathbf{k}'} \beta_{\mathbf{k}} - \alpha_{\mathbf{k}}^\dagger \alpha_{\mathbf{k}'}) S^- + \frac{1}{2} (\beta_{\mathbf{k}}^\dagger \beta_{\mathbf{k}'}^\dagger - \alpha_{\mathbf{k}'} \alpha_{\mathbf{k}}) S^+ \right] \right\}, \end{aligned} \quad (61)$$

where we have introduced

$$\begin{aligned} B_{\sigma\mathbf{k}} &= \frac{\tilde{J}_k}{N} \sum_{\mathbf{q}} \frac{E_{\mathbf{q}} + (v_{\mathbf{q}}^2 - u_{\mathbf{q}}^2) E_{\mathbf{k}}}{E_{\mathbf{q}}^2 - E_{\mathbf{k}}^2} (1 - 2\langle \alpha_{\mathbf{q}}^\dagger \alpha_{\mathbf{q}} \rangle) \\ B_{\bar{\sigma}\mathbf{k}} &= -\frac{2\tilde{J}_k}{N} \sum_{\mathbf{q}} \frac{u_{\mathbf{q}} v_{\mathbf{q}} E_{\mathbf{k}}}{E_{\mathbf{q}}^2 - E_{\mathbf{k}}^2} (1 - 2\langle \alpha_{\mathbf{q}}^\dagger \alpha_{\mathbf{q}} \rangle). \end{aligned} \quad (62)$$

The effective scattering in Eq. (61), which was obtained after the factorization, has the same operator structure as  $\mathcal{H}_{1,J}$  in Eq. (53). This property allows us to fix the coefficients  $\tilde{J}_k$  in such a way that all terms which have the operator structure of the original spin-fermion scattering are eliminated. For a non-singular  $\tilde{J}_k$ , the corresponding condition can be read off the first order transformation (since all other terms vanish in the thermodynamic limit). We find

$$\mathcal{H}_{1,J} + [X_J, \mathcal{H}_0] + [X_J, \mathcal{H}_{1,J}]_{2,\text{factorized}} = 0. \quad (63)$$

Note that  $[X_J, \mathcal{H}_0]$  has also the operator structure of  $\mathcal{H}_{1,J}$  and therefore has to be included in this step. If  $\tilde{J}_k$  becomes singular at some particular  $\mathbf{k}$ , the transformation has again to be summed up to infinity. This, however, only leads to modified prefactors appearing as sin- and cos-functions similar to Eq. (7)

Since the following discussion is very similar to the ones of a classical spin and a potential impurity, we for simplicity now focus on non-singular  $\tilde{J}_k$ . We calculate their values by numerically solving the implicit equation Eq. (63) for  $\tilde{J}_k$ . An approximate analytical solution can easily be obtained for states near the Fermi surface by a discussion similar to Sec. 3.1. For such states, we find  $C_1^+ = C_2^+ = 1$ ,  $C_1^- = C_2^- = 0$ ,  $B_{\sigma k} = B_{\sigma k'}$ , and  $B_{\bar{\sigma} k} = B_{\bar{\sigma} k'}$ . Using these simplifications, we obtain from Eqs. (53), (54), (61), and (62) the following expressions for states near the Fermi surface,

$$\begin{aligned} \mathcal{H}_{1,J} |_{|k|,|k'| \approx k_F} &= \frac{J}{2N} \sum_{kk'} (\alpha_k^\dagger \alpha_{k'} S_z - \beta_k^\dagger \beta_{k'} S_z + \alpha_k^\dagger \beta_{k'} S^- + \beta_k^\dagger \alpha_k S^+), \\ [X_J, \mathcal{H}_0] |_{|k|,|k'| \approx k_F} &= -\frac{1}{N} \sum_{kk'} \tilde{J}_k (\alpha_k^\dagger \alpha_{k'} S_z - \beta_k^\dagger \beta_{k'} S_z + \alpha_k^\dagger \beta_{k'} S^- + \beta_k^\dagger \alpha_k S^+), \\ [X_J, \mathcal{H}_{1,J}]_2 |_{|k|,|k'| \approx k_F} &= \\ \frac{J}{N} \sum_{kk'} \left\{ \frac{\tilde{J}_k}{N} \sum_q \frac{E_q + \frac{\Delta - \varepsilon_q}{E_q} E_k}{E_q^2 - E_k^2} (1 - 2\langle \alpha_q^\dagger \alpha_q \rangle) (\alpha_k^\dagger \alpha_{k'} S_z - \beta_k^\dagger \beta_{k'} S_z + \alpha_k^\dagger \beta_{k'} S^- + \beta_k^\dagger \alpha_k S^+) \right\}. \end{aligned} \quad (64)$$

Since all these expressions have the same operator form, we find that Eq. (63) translates to

$$\left[ \frac{J}{2} - \tilde{J}_k + \tilde{J}_k \frac{J}{N} \sum_q \frac{E_q + \frac{\Delta - \varepsilon_q}{E_q} E_k}{E_q^2 - E_k^2} (1 - 2\langle \alpha_q^\dagger \alpha_q \rangle) \right]_{|k| \approx k_F} = 0. \quad (65)$$

Thus, the solution of the renormalized exchange coupling for states near the Fermi surface reads

$$\tilde{J}_k |_{|k| \approx k_F} = \frac{J/2}{1 - \frac{J}{N} \sum_q \frac{E_q + \frac{\Delta - \varepsilon_q}{E_q} E_k}{E_q^2 - E_k^2} (1 - 2\langle \alpha_q^\dagger \alpha_q \rangle)}. \quad (66)$$

Its form resembles the form of the coefficients of a unitary transformation involving bound states with a possible singular behavior as discussed in the previous sections.

### Second transformation step

Finally, similar to the classical spin case, we integrate out the remaining quadratic part  $\tilde{\mathcal{H}}_{1,J}$  of the effective scattering  $\tilde{\mathcal{H}}_{1,J} = [X_J, \mathcal{H}_{1,J}]_1$  where the commutator is explicitly given by Eq. (59). Our starting point for the second transformation step is

$$\begin{aligned} \tilde{\mathcal{H}}_{1,J} &= -\frac{J}{2} S(S+1) \frac{1}{N} \sum_{kk'} \left\{ [C_1^+(\mathcal{J}_{\sigma k} + \mathcal{J}_{\sigma k'}) + C_2^+(\mathcal{J}_{\bar{\sigma} k} + \mathcal{J}_{\bar{\sigma} k'})] (\alpha_k^\dagger \alpha_{k'} + \beta_k^\dagger \beta_{k'}) \right. \\ &\quad \left. - [C_2^-(\mathcal{J}_{\sigma k} - \mathcal{J}_{\sigma k'}) - C_1^-(\mathcal{J}_{\bar{\sigma} k} + \mathcal{J}_{\bar{\sigma} k'})] (\alpha_k^\dagger \beta_{k'}^\dagger + \beta_{k'} \alpha_k) \right\}, \end{aligned} \quad (67)$$

with the renormalized Green's functions (60) and the renormalized exchange coupling  $\tilde{J}_k$ . These quantities were determined numerically within the previous step. According to the same procedure as carried out for the classical case, we now apply a second unitary transformation to eliminate the non-diagonal scattering terms described by  $\tilde{\mathcal{H}}_{1,J}$ . Comparing the expressions of the effective scattering in the classical spin case, Eq. (37), with the corresponding expression for the

quantum spin case, Eq. (67), one immediately finds that the same ansatz (38) for the generator can be used also in the present case,

$$\begin{aligned} \tilde{X}_J = & -\frac{1}{N} \sum_{\mathbf{k}\mathbf{k}'} \frac{A_{\mathbf{k},J} + A_{\mathbf{k}',J}}{E_{\mathbf{k}} - E_{\mathbf{k}'}} (u_{\mathbf{k}}u_{\mathbf{k}'} + v_{\mathbf{k}}v_{\mathbf{k}'} + u_{\mathbf{k}}v_{\mathbf{k}'} + u_{\mathbf{k}'}v_{\mathbf{k}}) (\alpha_{\mathbf{k}}^\dagger \alpha_{\mathbf{k}'} + \beta_{\mathbf{k}}^\dagger \beta_{\mathbf{k}'}) \\ & - \frac{1}{N} \sum_{\mathbf{k}\mathbf{k}'} \left[ (u_{\mathbf{k}}v_{\mathbf{k}'} - u_{\mathbf{k}'}v_{\mathbf{k}}) \frac{A_{\mathbf{k},J} - A_{\mathbf{k}',J}}{E_{\mathbf{k}} + E_{\mathbf{k}'}} - (u_{\mathbf{k}}u_{\mathbf{k}'} - v_{\mathbf{k}}v_{\mathbf{k}'}) \frac{A_{\mathbf{k},J} + A_{\mathbf{k}',J}}{E_{\mathbf{k}} + E_{\mathbf{k}'}} \right] (\alpha_{\mathbf{k}}^\dagger \beta_{\mathbf{k}'}^\dagger - \beta_{\mathbf{k}'} \alpha_{\mathbf{k}}). \end{aligned} \quad (68)$$

As in Sec. 3.1, we evaluate the unitary transformation by calculating at first the commutator  $[\tilde{X}_J, \tilde{\mathcal{H}}_{1,J}]$  and then summing up all higher orders to sin- and cos-functions. We numerically solve the resulting expression for the coefficients  $A_{\mathbf{k},J}$  such that the Hamiltonian becomes  $\mathbf{k}$ -diagonal. We obtain again a singular result for  $A_{\mathbf{k},J}$  indicating the formation of a bound state. As in the classical spin case, we call the corresponding quantum number  $\mathbf{k}_0$ . Comparing the prefactors of the operator terms in Eqs. (67) and (37), we simply can replace  $\frac{J}{2}S^2G_{\sigma\mathbf{k}}$  with  $S(S+1)\mathcal{J}_{\sigma\mathbf{k}}$ .

Following Sec. 3.1, we again focus on states near the Fermi surface to obtain an approximate analytical solution. Similar to our earlier result in Eq. (41), we now obtain the following explicit solution of the singular coefficient  $A_{\mathbf{k}_0,J}$  of the second unitary transformation

$$A_{\mathbf{k}_0,J} = \frac{-\frac{J}{2}S(S+1)(\mathcal{J}_{\sigma\mathbf{k}_0} + \mathcal{J}_{\bar{\sigma}\mathbf{k}_0})}{1 - \frac{J}{2}S(S+1)(\mathcal{J}_{\sigma\mathbf{k}_0} + \mathcal{J}_{\bar{\sigma}\mathbf{k}_0})(G_{\sigma\mathbf{k}_0} + G_{\bar{\sigma}\mathbf{k}_0})}, \quad (69)$$

where the dimensionless coefficient  $\mathcal{J}_{\sigma\mathbf{k}_0}$  is given by Eq. (60) considered at  $E_{\mathbf{k}} = \omega_0$ . The singularity which arises from a vanishing denominator leads again to the YSR bound state. It fulfills the equation,

$$1 = \frac{J}{2} (\nu_0 \pi)^2 S(S+1) \frac{\Delta + \omega_0}{\Delta - \omega_0} \tilde{J}_{\mathbf{k}_0}, \quad (70)$$

where  $\tilde{J}_{\mathbf{k}_0}$  is the renormalized magnetic exchange coupling  $\tilde{J}_{\mathbf{k}}$  from the first transformation step considered at the bound state  $\mathbf{k}_0$ . Since our numerics shows that  $\mathbf{k}_0$  is part of the normal state Fermi surface we can find an approximate explicit expression for  $\tilde{J}_{\mathbf{k}_0}$  from Eq. (66) where the energy  $E_{\mathbf{k}}$  of the state  $\mathbf{k}$  is replaced with the energy  $\omega_0$  of the bound state,

$$\tilde{J}_{\mathbf{k}_0} = \frac{J/2}{1 - \frac{J}{N} \sum_{\mathbf{q}} \frac{E_{\mathbf{q}} + \frac{\Delta - \varepsilon_{\mathbf{q}}}{E_{\mathbf{q}}} \omega_0}{E_{\mathbf{q}}^2 - \omega_0^2} (1 - 2\langle \alpha_{\mathbf{q}}^\dagger \alpha_{\mathbf{q}} \rangle)}. \quad (71)$$

Note that the expectation value  $\langle \alpha_{\mathbf{q}}^\dagger \alpha_{\mathbf{q}} \rangle$  again depends on  $\omega_0$ . Eq. (70) therefore has to be solved self-consistently for  $\omega_0$ , which implies a temperature-dependence of  $\omega_0$ . Corresponding numerical results are shown in Appendix A. Eq. (70) has a solution for  $\omega_0$  only in the superconducting state, i. e. if  $\Delta \neq 0$ , which reads

$$\omega_0 = \Delta \frac{1 - \frac{J}{2} \tilde{J}_{\mathbf{k}_0} (\nu_0 \pi)^2 S(S+1)}{1 + \frac{J}{2} \tilde{J}_{\mathbf{k}_0} (\nu_0 \pi)^2 S(S+1)}. \quad (72)$$

Note that due to the factor  $S(S+1)$  the energy  $\omega_0$  in the quantum spin case is somewhat renormalized in comparison with the classical spin case as given by Eq. (46). This behavior is also studied in some detail in Appendix A.

In Fig. 4 we show the result of the self-consistent solution of Eq. (72) at  $T = 0$  for the energy  $\omega_0$  as a function of the Kondo temperature  $k_B T_K$ . Here the Kondo temperature is varied by changing the exchange coupling parameter  $J$ . The relationship between  $T_K$  and  $J$  is

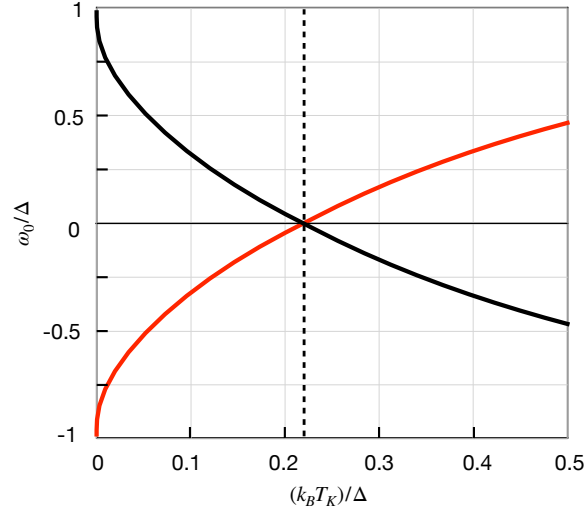


Figure 4: Energy of the YSR state as a function of the Kondo temperature. The crossing point of the two branches  $\pm\omega_0$  of the bound state excitation marks the transition from the YSR regime to the Kondo singlet state.

$k_B T_K = W \sqrt{J\nu_0} \exp\left(-\frac{1}{J\nu_0}\right)$ . The energy of the second YSR excitation at  $-\omega_0$  is also shown (red line). One clearly recognizes the behavior known from former numerical studies [6,27] including the crossing at  $\omega_0 = 0$  (dashed line) which marks the transition from a weak coupling regime at low  $T_K$  to a strong coupling regime at larger  $T_K$  where the Kondo physics becomes significant. Our numerical solution shows that the strong coupling regime is characterized by a singularity in the renormalized exchange coupling  $\tilde{J}_k$ . This is already seen in its approximate analytical solution given by Eq. (66) where the denominator can become zero depending on external parameters.

### 3.2.2 Transformation of operators

The calculation of observables again requires us to transform the quasiparticle operators using the same transformations that we applied to the Hamiltonian, see Eqs. (2) and (3). For the present case of the quantum spin, we apply the two subsequent transformation steps as described above with the generators  $X_J$  and  $\tilde{X}_J$ . The corresponding coefficients of the generators,  $\tilde{J}_k$  and  $A_{k,J}$ , and the renormalized one-particle energies  $\tilde{E}_k$  are calculated numerically as a result of the transformation of the Hamiltonian. For a solution leading to one singular state  $\mathbf{k}_0$  where  $\tilde{E}_{\mathbf{k}_0} = \omega_0$  the transformation of the quasiparticle operator reads in total

$$\begin{aligned} \tilde{\alpha}_{\mathbf{k},J}^\dagger = & \cos \phi_{\mathbf{k},J1} \left\{ \cos \phi_{\mathbf{k},J2} \alpha_{\mathbf{k}}^\dagger - \sin \phi_{\mathbf{k},J2} \left( \frac{u_{\mathbf{k}} + v_{\mathbf{k}}}{\sqrt{2}} \alpha_{\mathbf{k}_0}^\dagger + \frac{u_{\mathbf{k}} - v_{\mathbf{k}}}{\sqrt{2}} \beta_{\mathbf{k}_0} \right) \right\} \\ & + \frac{\sin \phi_{\mathbf{k},J1}}{\sqrt{S(S+1)}} \left\{ \frac{u_{\mathbf{k}} + v_{\mathbf{k}}}{\sqrt{2}} (S_z \alpha_{\mathbf{k}_0}^\dagger - S^+ \beta_{\mathbf{k}_0}^\dagger) + \frac{u_{\mathbf{k}} - v_{\mathbf{k}}}{\sqrt{2}} (-S_z \beta_{\mathbf{k}_0} + S^+ \alpha_{\mathbf{k}_0}) \right\}, \end{aligned} \quad (73)$$

and an analog expression is also obtained for  $\tilde{\beta}_{\mathbf{k},J}^\dagger$ . The phase coefficients  $\phi_{\mathbf{k},J1}$  and  $\phi_{\mathbf{k},J2}$  referring to the two transformation steps are given by

$$\tan \phi_{\mathbf{k},J1} = \frac{1}{N} \sqrt{S(S+1) \sum_{\mathbf{q}(\neq \mathbf{k})} \left( \frac{J + \tilde{J}_{\mathbf{q}}}{\tilde{E}_{\mathbf{k}} - \tilde{E}_{\mathbf{q}}} \right)^2} \quad \text{and} \quad \tan \phi_{\mathbf{k},J2} = \frac{1}{N} \sqrt{\sum_{\mathbf{q}(\neq \mathbf{k})} \left( \frac{\tilde{J}_{\mathbf{k}} + A_{\mathbf{q},J}}{\tilde{E}_{\mathbf{k}} - \tilde{E}_{\mathbf{q}}} \right)^2}. \quad (74)$$

The above transformation (73) allows us to calculate any expectation value. For example, the self-consistency loop to obtain the renormalized exchange coupling  $\tilde{J}_{\mathbf{k}}$  requires to calculate the expectation value  $\langle \alpha_{\mathbf{k}}^{\dagger} \alpha_{\mathbf{k}} \rangle$ . Using again the invariance of the trace under unitary transformations we simply can write  $\langle \alpha_{\mathbf{k}}^{\dagger} \alpha_{\mathbf{k}} \rangle = \langle \tilde{\alpha}_{\mathbf{k}}^{\dagger} \tilde{\alpha}_{\mathbf{k}} \rangle_{\tilde{\mathcal{H}}}$ . Since the final effective Hamiltonian  $\tilde{\mathcal{H}}$  is diagonal, this expectation value is easily obtained after inserting Eq. (73).

### 3.2.3 Discussion of the quasiparticle nature

Eq. (73) shows that the fully transformed quasiparticle operators contain two types of contributions. (i) The term proportional to  $\cos \phi_{\mathbf{k},J1} \cos \phi_{\mathbf{k},J2} \alpha_{\mathbf{k}}^{\dagger}$  corresponds to propagating quasiparticle excitations living at the bare dispersive energies  $E_{\mathbf{k}}$ . They should consequently be interpreted as the usual dispersive Bogoliubov quasiparticle excitations. (ii) All remaining terms are related to the bound state, which is heralded by the appearance of the bound state quantum number  $\mathbf{k}_0$ . (Also, as we show below, all of these terms give rise to an excitation with the bound state energy  $\omega_0$ ).

The explicit form of the quasiparticle excitation operators furthermore depends on the phase factors  $\phi_{\mathbf{k},J1}$  and  $\phi_{\mathbf{k},J2}$ . The values of these phases change when the bound state energy  $\omega_0$  crosses zero. This means that the operator content of our quasiparticle excitation operators changes when the bound state changes between being occupied and being empty.

Let us first turn to the regime of weak exchange couplings  $J$  such that  $\omega_0 > 0$ . Our numerical analysis shows that the main contribution to the bound state weight then occurs for  $\tilde{\alpha}_{\mathbf{k},J}^{\dagger}$  with  $|\mathbf{k}|$  close to the Fermi momentum  $k_F$ . For these states, we find  $\phi_{\mathbf{k},J1} = 0$  and  $\phi_{\mathbf{k},J2} = \pi/4$ , while  $u_{\mathbf{k}} = v_{\mathbf{k}} = 1/\sqrt{2}$ . Using Eq. (73), the quasiparticle operators then have the form

$$(\tilde{\alpha}_{\mathbf{k},J}^{\dagger})_{\omega_0 > 0} = \frac{1}{\sqrt{2}} \alpha_{\mathbf{k}_F}^{\dagger} - \frac{1}{\sqrt{2}} \alpha_{\mathbf{k}_0}^{\dagger}. \quad (75)$$

which exactly agrees with the structure of the quasiparticle in the classical spin case as given by Eq. (49). The bound state contribution  $\alpha_{\mathbf{k}_0}^{\dagger}$  is in that sense directly connected to a classical YSR state. We therefore denote the regime  $\omega_0 > 0$  as the YSR regime.

For  $\omega_0 < 0$ , we find that for states close to the Fermi momentum, the first phase factor switches its value to  $\phi_{\mathbf{k},J1} = \pi/4$ , whereas the second phase factor keeps its value of  $\phi_{\mathbf{k},J2} = \pi/4$ . This switching is caused by a singular behavior of the renormalized exchange coupling  $\tilde{J}_{\mathbf{k}}$  for states near the normal state Fermi surface. As can be read off Eq. (73), this leads to a qualitatively new contribution to the quasiparticle operator which has a completely different structure involving the impurity spin operators,

$$(\tilde{\alpha}_{\mathbf{k},J}^{\dagger})_{\omega_0 < 0} = \frac{1}{2} \alpha_{\mathbf{k}}^{\dagger} - \frac{1}{2} \alpha_{\mathbf{k}_0}^{\dagger} + \frac{1}{\sqrt{2} \sqrt{S(S+1)}} (S_z \alpha_{\mathbf{k}_0}^{\dagger} - S^+ \beta_{\mathbf{k}_0}^{\dagger}). \quad (76)$$

The bound state contribution now takes the form of a composite fermion build from a superconducting quasiparticle and the local quantum spin. Introducing the spinor notation  $\tilde{\alpha}_{\nu \mathbf{k},J}^{\dagger}$  where  $\tilde{\alpha}_{\uparrow \mathbf{k},J}^{\dagger} = \tilde{\beta}_{\mathbf{k},J}^{\dagger}$  and  $\tilde{\alpha}_{\downarrow \mathbf{k},J}^{\dagger} = \tilde{\alpha}_{\mathbf{k},J}^{\dagger}$ , we find that Eq. (76) can be rewritten as

$$(\tilde{\alpha}_{\nu \mathbf{k},J}^{\dagger})_{\omega_0 < 0} = \frac{\alpha_{\nu \mathbf{k}_F}^{\dagger} - \alpha_{\nu \mathbf{k}_0}^{\dagger}}{2} + \frac{1}{\sqrt{2S(S+1)}} \sum_{\mu} (\vec{S} \cdot \vec{\sigma})_{\nu\mu} \alpha_{\mu \mathbf{k}_0}^{\dagger}. \quad (77)$$

This form of the bound state operator is reminiscent of the well-known quasiparticle operator in the Kondo effect [36, 37]. We therefore denote the regime  $\omega_0 > 0$  as the Kondo regime.

### 3.2.4 Spectral function

Finally, we are again interested in the one-particle spectral function. Using Eq. (73), we obtain the following expression for  $\mathbf{k} \neq \mathbf{k}_0$ ,

$$\begin{aligned} \Im G(\mathbf{k}, \mathbf{k}, \omega) &= \frac{1}{2} \cos^2 \phi_{\mathbf{k},J1} \cos^2 \phi_{\mathbf{k},J2} \left( 1 \pm \frac{\varepsilon_{\mathbf{k}}}{E_{\mathbf{k}}} \right) \delta(\pm E_{\mathbf{k}} - \omega) \\ &+ \frac{1}{2} \left( \cos^2 \phi_{\mathbf{k},J1} \sin^2 \phi_{\mathbf{k},J2} + \sin^2 \phi_{\mathbf{k},J1} \right) \left( 1 \pm \frac{\varepsilon_{\mathbf{k}} \Delta}{E_{\mathbf{k}}^2} \right) \delta(\pm \omega_0 - \omega). \end{aligned} \quad (78)$$

We find that the spectral density for  $\mathbf{k} \neq \mathbf{k}_0$  is mainly associated with dispersive conduction electrons. Note that spectral weight is transferred from the coherent excitation to the excitation of the bound state at  $\pm \omega_0$  leading (as in the classical spin case) to a  $\mathbf{k}$  dependent intensity of the excitation peaks. Further note that according to Eq. (74), the numerical solutions of the renormalized exchange coupling and the coefficient  $A_{\mathbf{k}}$  are contained in the phases  $\phi_{\mathbf{k},J1}$  and  $\phi_{\mathbf{k},J2}$ . For  $\mathbf{k} = \mathbf{k}_0$ , we obtain

$$\begin{aligned} \Im G(\mathbf{k}_0, \mathbf{k}_0, \omega) &= \frac{1}{2N} \sum_{\mathbf{k}(\neq \mathbf{k}_0)} \left[ \cos^2 \phi_{\mathbf{k},J1} \cos^2 \phi_{\mathbf{k},J2} \left( 1 \pm \frac{\varepsilon_{\mathbf{k}} \Delta}{E_{\mathbf{k}}^2} \right) \delta(\pm \omega_0 - \omega) \right. \\ &\left. + \left( \cos^2 \phi_{\mathbf{k},J1} \sin^2 \phi_{\mathbf{k},J2} + \sin^2 \phi_{\mathbf{k},J1} \right) \left( 1 \pm \frac{\varepsilon_{\mathbf{k}}}{E_{\mathbf{k}}} \right) \delta(\pm E_{\mathbf{k}} - \omega) \right]. \end{aligned} \quad (79)$$

To illustrate the spectral function, we numerically evaluate Eq. (78) together with a fully self-consistent solution of the renormalized energies and expectation values. We consider three different values of  $J/\Delta$  corresponding to a rather weak coupling in the YSR regime,  $J/\Delta = 20$ , the intermediate coupling  $J/\Delta = 55$ , and a large value  $J/\Delta = 120$  in the Kondo regime.

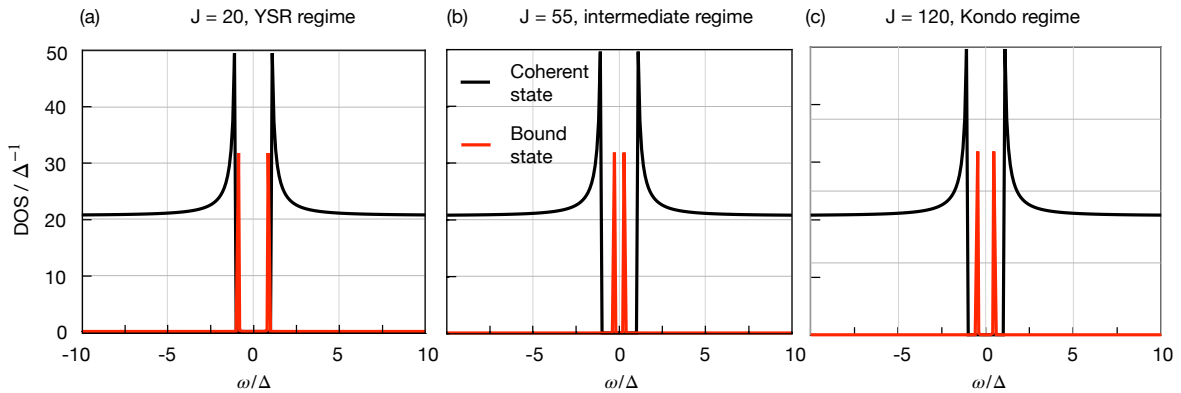


Figure 5: Total density of states for three different values of  $J$  in an energy region around the Fermi level. These results were obtained by momentum summation of both parts  $\mathbf{k} = \mathbf{k}_0$  and  $\mathbf{k} \neq \mathbf{k}_0$  of the spectral function according to Eqs. (78) and (79). The superconducting gap is clearly seen. The bound state inside the gap is shown in a different color. The energy integral over the whole bandwidth leads to the total number of states  $N$  (for all values of  $J$ ).

First, we turn to the momentum-integrated spectral function including the bound state quantum number  $\mathbf{k}_0$ . Fig. 5 shows the spectral density in a narrow region around the Fermi level. The

superconducting gap and a density of states of the conduction electrons are not found to vary noticeably with  $J$ . The excitation peak of the YSR state (shown in red color), on the other hand, moves in energy as  $J$  changes. As a crosscheck, we verified that the energy integral over the total density of states yields the total number of states  $N$ .

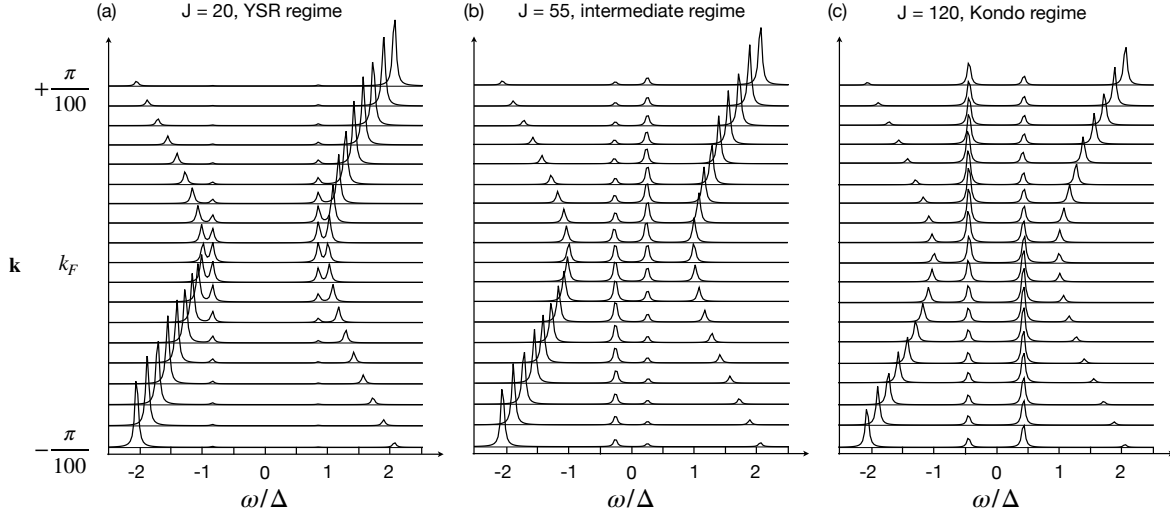


Figure 6: Spectral functions for the same parameters as in Fig. 5 but only for  $\mathbf{k} \neq \mathbf{k}_0$ . The level broadening is chosen to the value  $\eta = 0.03\Delta$ . The bound state at  $\omega_0$  becomes extended in momentum space and the distribution of the spectral weight in momentum space gets inverted when the Kondo regime is entered.

More interesting is the momentum-resolved spectral function, which we now discuss for  $\mathbf{k} \neq \mathbf{k}_0$ . It is shown in Fig. 6. In the weak coupling YSR regime at  $J/\Delta = 20$ , the spectrum is composed of a dispersive excitation and a YSR bound state located close to the gap edge. The dispersive excitation loses spectral weight once the momentum approaches  $k_F$ , while the spectral weight of the YSR state increases. In contrast to the case of a classical spin, the intensity distribution of the YSR state is not particle-hole symmetric.

This can be seen even more clearly in Fig. 6(b), where a larger value of  $J$  is considered. The two YSR peaks also move closer together, and become somewhat more intense. At the same time, the coherent excitation weakens. The YSR state now also has a somewhat larger extent in momentum space, but still remains relatively close to  $k_F$ .

If, finally, the exchange coupling is increased even more, the YSR states cross zero energy. As shown in Fig. 6(c), the bound state spectral weight coming from momenta  $\mathbf{k} \neq \mathbf{k}_0$  is now much larger than that in the weak coupling YSR regime. The numerical evaluation of this spectral weight as a function of  $J$  (not shown here) reveals a jump at the transition point which agrees well with former studies [27]. Furthermore, the distribution of spectral weight in momentum space is particle-hole-reversed as compared to the weak coupling-regime.

## 4 Conclusion

We have presented a new semi-analytical approach to solve a model Hamiltonian describing a local quantum spin coupled to a superconducting substrate. Postponing a detailed derivation to



a subsequent publication, we stress that our method can straightforwardly be extended to larger numbers of impurities. The basic idea of our approach is to eliminate the scattering interaction between electrons and the impurity by unitary transformations that yields a diagonal renormalized Hamiltonian. In this process, bound states manifest themselves as singularities in the unitary transformation.

We first illustrated the approach with the simple example of a potential impurity in a spinless electron bath, and showed that we reproduce the results of the usual t-matrix approach. We then applied our method to both the cases of a classical and a quantum spin coupled to a superconductor. In the case of a classical spin, our approach agrees with alternative analytical solutions to the problem, and in particular fully captures Yu-Shiba-Rusinov bound states. In the case of a quantum spin coupled to a BCS *s*-wave superconductor, our method shows good agreement with fully numerical studies and STM experiments. In addition, we showed that our approach directly yields access to momentum-resolved observables, which for example are important in the context of ARPES-experiments.

In contrast to purely numerical approaches, our method also allows for detailed analytical insights. This power of our approach is rooted in the fact that bound states manifest themselves as singularities, and that it is therefore sufficient to extract this singular behavior from the full picture to investigate bound state physics. This for example allows us to explicitly construct bound state quasiparticle operators, which in turn reveals how increasing quantum fluctuations of the local spin pushes the bound state from a YSR-like form to a Kondo-like expression.

## Acknowledgements

We would like to thank K.W. Becker for helpful discussions.

**Funding information** This project has received funding from the Deutsche Forschungsgemeinschaft via the Emmy Noether Programme ME4844/1-1 (project id 327807255), the Collaborative Research Center SFB 1143 (project id 247310070), and the Cluster of Excellence on Complexity and Topology in Quantum Matter ct.qmat (EXC 2147, project id 390858490).

## A Effect of spin and temperature

In Fig. 7 we show results of the bound state energy  $\omega_0$  as a function of the size  $S$  of the local spin (panel (a)) and as a function of the temperature  $T$  (panel(b)) where  $T$  is always kept below the critical temperature  $T_c$ . Clearly seen is the strong reduction of  $\omega_0$  with  $S$  in all regimes. As expected the most significant effect of quantum fluctuations is obtained at small values of  $S$  where the energy  $\omega_0$  deviates mostly from the classical spin limit (dashed lines). However, in the YSR regime the effect of the quantum nature of the spin is indeed rather weak but it extends over a wider range of  $S$  than in the Kondo regime. Here the effect is large mainly in the  $S = 1/2$  case.

Furthermore, in Fig. 7(b) we have calculated the influence of the temperature  $T$  in the two different regimes at  $J/\Delta = 20$  and  $J/\Delta = 120$ . In agreement with the numerical results from Ref. [6] we find a characteristic temperature effect where in the YSR regime the bound state energy is shifted to smaller values. This effect becomes inverted in the Kondo regime where the shift is smaller but the energy increases with temperature.



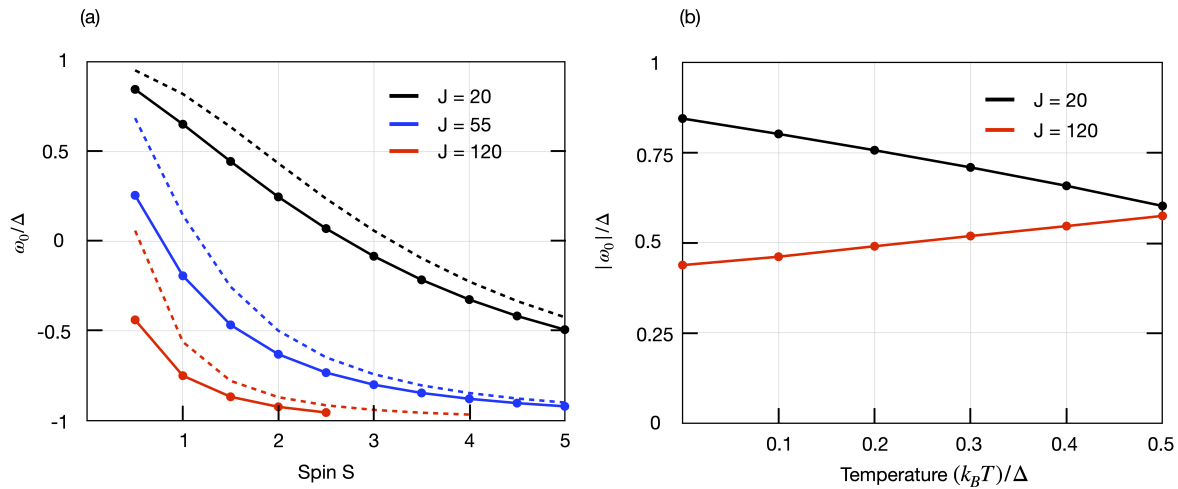


Figure 7: Behavior of the bound state energy of a quantum spin under variation of different parameters. (a) Variation of the spin for the three different values of  $J$  discussed above. The corresponding results for the classical spin are also shown (dashed lines). In all regimes  $\omega_0$  approaches the value of the classical spin case in the limit of large  $S$ . (b) Variation of the temperature. In agreement with former numerical studies [6] the YSR state energy decreases with temperature while in the Kondo regime it slightly increases.

## References

- [1] L. Yu, *Acta Physica Sinica* **21**, 75 (1965).
- [2] H. Shiba, *Classical Spins in Superconductors*, *Prog. Theoret. Phys.* **40**, 435 (1968), doi:<https://doi.org/10.1143/PTP40.435>.
- [3] A. I. Rusinov, *Superconductivity near a Paramagnetic Impurity* *JETP Lett.* **9**, 85 (1969).
- [4] J. Kondo, *Resistance Minimum in Dilute Magnetic Alloys* *Prog. Theor. Phys.* **32**, 37 (1964), doi:<https://doi.org/10.1143/PTP32.37>.
- [5] R. Wang, W. Su, J.-X. Zhu, C. S. Ting, H. Li, C. Chen, B. Wang, and X. Wang, *Kondo Signatures of a Quantum Magnetic Impurity in Topological Superconductors* *Phys. Rev. Lett.* **122**, 087001 (2019), doi:<https://doi.org/10.1103/PhysRevLett.122.087001>.
- [6] C. Liu, Y. Huang, Y. Chen, C. S. Ting, *Temperature-dependent spectral function of a Kondo impurity in an s-wave superconductor*, *Phys. Rev. B* **99**, 245139 (2018), doi:[10.1103/PhysRevB.99.174502](https://doi.org/10.1103/PhysRevB.99.174502).
- [7] M. I. Salkola, A. V. Balatsky, and J. R. Schrieffer, *Spectral properties of quasiparticle excitations induced by magnetic moments in superconductors* *Phys. Rev. B* **55**, 12648 (1997), doi:<https://doi.org/10.1103/PhysRevB.55.12648>.
- [8] R. S. Deacon, Y. Tanaka, A. Oiwa, R. Sakano, K. Yoshida, K. Shibata, K. Hirakawa, and S. Tarucha, *Tunneling Spectroscopy of Andreev Energy Levels in a Quantum Dot Coupled to a Superconductor*, *Phys. Rev. Lett.* **104**, 076805 (2010), doi:<https://doi.org/10.1103/PhysRevLett.104.076805>.

- [9] K. J. Franke, G. Schulze, J. I. Pascual, *Competition of Superconducting Phenomena and Kondo Screening at the Nanoscale*, Science **332**, 6032 (2011), doi:[10.1126/science.1202204](https://doi.org/10.1126/science.1202204).
- [10] B. W. Heinrich, J. I. Pascual, K. J. Franke, *Single magnetic adsorbates on s-wave superconductors*, Progress in Surface Science **93**, 1 (2018), doi:<https://doi.org/10.1016/j.progsurf.2018.01.001>.
- [11] A. Yazdani, B. A. Jones, C. P. Lutz, M. F. Crommie, and D. M. Eigler, *Probing the Local Effects of Magnetic Impurities on Superconductivity*, Science **275**, 1767 (1997), doi:[10.1126/science.275.5307.1767](https://doi.org/10.1126/science.275.5307.1767).
- [12] S.-H. Ji, et.al., *High-Resolution Scanning Tunneling Spectroscopy of Magnetic Impurity Induced Bound States in the Superconducting Gap of Pb Thin Films*, Phys. Rev. Lett. **100**, 226801 (2008), doi:<https://doi.org/10.1103/PhysRevLett.100.226801>.
- [13] M. Flatte and D. Reynolds, *Local spectrum of a superconductor as a probe of interactions between magnetic impurities*, Phys. Rev. B **61**, 14810 (2000), doi:<https://doi.org/10.1103/PhysRevB.61.14810>.
- [14] D. Morr and N. Stavropoulos, *Quantum interference between impurities: Creating novel many-body states in s-wave superconductors*, Phys. Rev. B **67**, 020502(R) (2003), doi:<https://doi.org/10.1103/PhysRevB.67.020502>.
- [15] T. Meng, J. Klinovaja, S. Hoffman, P. Simon, and D. Loss, *Superconducting gap renormalization around two magnetic impurities: From Shiba to Andreev bound states*, Phys. Rev. B **92**, 125422 (2015), doi:<https://doi.org/10.1103/PhysRevB.92.064503>.
- [16] S. Hoffman, J. Klinovaja, T. Meng, and D. Loss, *Impurity-induced quantum phase transitions and magnetic order in conventional superconductors: Competition between bound and quasiparticle states*, Phys. Rev. B **92**, 064503 (2015), doi:<https://doi.org/10.1103/PhysRevB.92.125422>.
- [17] S. Nadj-Perge, I. K. Drozdov, B. A. Bernevig, and A. Yazdani, *Proposal for realizing Majorana fermions in chains of magnetic atoms on a superconductor*, Phys. Rev. B **88**, 020407(R) (2013), doi:<https://doi.org/10.1103/PhysRevB.88.020407>.
- [18] F. Pientka, L. I. Glazman, and F. V. Oppen, *Topological superconducting phase in helical Shiba chains* Phys. Rev. B **88**, 155420 (2013), doi:<https://doi.org/10.1103/PhysRevB.88.155420>.
- [19] S. Nadj-Perge, I. K. Drozdov, J. Li, H. Chen, S. Jeon, J. Seo, A. H. MacDonald, B. A. Bernevig, and A. Yazdani, *Observation of Majorana fermions in ferromagnetic atomic chains on a superconductor*, Science **346**, 602 (2014), doi:[10.1126/science.1259327](https://doi.org/10.1126/science.1259327).
- [20] J. Li, H. Chen, I. K. Drozdov, A. Yazdani, B. A. Bernevig, and A. H. MacDonald, *Topological superconductivity induced by ferromagnetic metal chains*, Phys. Rev. B **90**, 235433 (2014), doi:<https://doi.org/10.1103/PhysRevB.90.235433>.
- [21] A. Martin-Rodero and A. L. Yeyati, *The Andreev states of a superconducting quantum dot: mean field vs exact numerical results*, Journal of Physics: Condensed Matter **24**, 385303 (2012), doi:[10.1088/0953-8984/24/38/385303](https://doi.org/10.1088/0953-8984/24/38/385303).

- [22] M. Zonda, V. Pokorny, V. Janis, and T. Novotny, *Perturbation theory of a superconducting  $0 - \pi$  impurity quantum phase transition*, Scientific Reports **5**, 8821 (2015), doi:<https://www.nature.com/articles/srep08821.pdf?origin=ppub>.
- [23] M. Zonda, V. Pokorny, V. Janis, and T. Novotny, *Perturbation theory for an Anderson quantum dot asymmetrically attached to two superconducting leads*, Phys. Rev. B **93**, 024523 (2016), doi:<https://doi.org/10.1103/PhysRevB.93.024523>.
- [24] T. Meng, S. Florens, and P. Simon, *Self-consistent description of Andreev bound states in Josephson quantum dot devices*, Phys. Rev. B **79**, 224521 (2009), doi:<https://doi.org/10.1103/PhysRevB.79.224521>.
- [25] R. Maurand, T. Meng, E. Bonet, S. Florens, L. Marty, and W. Wernsdorfer, *First-Order  $0 - \pi$  Quantum Phase Transition in the Kondo Regime of a Superconducting Carbon-Nanotube Quantum Dot*, Phys. Rev. X **2**, 011009 (2012).
- [26] H. Shiba, K. Satori, O. Sakai, and Y. Shimizu, *Numerical renormalization group study of the Kondo effect in superconductors* Physica B: Condensed Matter **186-188**, 239 (1993), doi:[https://doi.org/10.1016/0921-4526\(93\)90540-M](https://doi.org/10.1016/0921-4526(93)90540-M).
- [27] O. Sakai, Y. Shimizu, H. Shiba, K. Satori, *Numerical Renormalization Group Study of Magnetic Impurities in Superconductors. II. Dynamical Excitation Spectra and Spatial Variation of the Order Parameter*, J. Phys. Soc. Jpn. **62**, 3181 (1993), doi:<https://doi.org/10.1143/JPSJ.62.3181>.
- [28] J. Bauer, A. Oguri, and A. C. Hewson, *Spectral properties of locally correlated electrons in a Bardeen-Cooper-Schrieffer superconductor* Journal of Physics: Condensed Matter **19**, 486211 (2007), doi:<https://iopscience.iop.org/article/10.1088/0953-8984/19/48/486211/meta>.
- [29] S. D. Glazek and K. G. Wilson, *Renormalization of Hamiltonians* Phys. Rev. D **48**, 5863 (1993), doi:<https://doi.org/10.1103/PhysRevD.48.5863>.
- [30] F. J. Wegner, *Flow-equations for Hamiltonians* Ann. Phys. (Leipzig) **506**, 77 (1994), doi:<https://doi.org/10.1002/andp.19945060203>.
- [31] S. Sykora, A. Hübsch, K. W. Becker, *Generalized diagonalization scheme for many-particle systems*, Phys. Rev. B **102**, 165122 (2020), doi:<https://doi.org/10.1103/PhysRevB.102.165122>.
- [32] A. V. Balatsky, I. Vekhter, and Jian-Xin Zhu, *Impurity-induced states in conventional and unconventional superconductors*, Rev. Mod. Phys. **78**, 373 (2006), doi:<https://doi.org/10.1103/RevModPhys.78.373>.
- [33] R. Zwanzig, *Nonequilibrium Statistical Mechanics 3rd ed.*, Oxford University Press, New York (2001).
- [34] H. Grabert, *Projection operator techniques in nonequilibrium statistical mechanics*, Springer Tracts in Modern Physics **95** (1982).
- [35] N. Hatter, B. W. Heinrich, D. Rolf, K. J. Franke, *Scaling of Yu-Shiba-Rusinov energies in the weak-coupling Kondo regime*, Nature Communications **8**, 2016 (2017), doi:<https://doi.org/10.1038/s41467-017-02277-7>.

- [36] M. Maltseva, M. Dzero, P. Coleman, *Electron Cotunneling into a Kondo Lattice*, Phys. Rev. Lett. **103**, 206402 (2009), doi:<https://doi.org/10.1103/PhysRevLett.103.206402>
- [37] S. Sykora, K. W. Becker, *Many-body approach to Luttinger's theorem for the Kondo lattice*, Phys. Rev. B **98**, 174502 (2019), doi:<https://doi.org/10.1103/PhysRevB.98.245139>.